

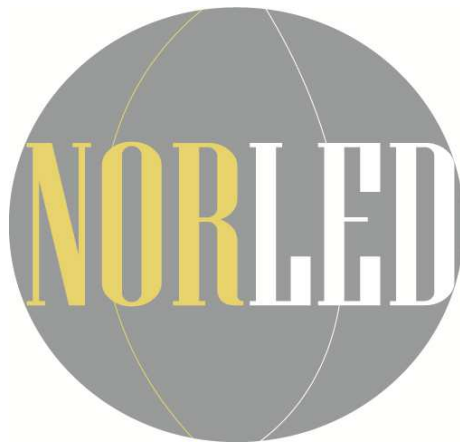
# **Final Scientific Report**

N-Inner (ii) project

**NORLED** - Northern Light Emitting Diode initiative

January 2014

Mikael Syväjärvi, Haiyan Ou, Peter Wellmann



## **Abstract**

The NORLED project initiated a new research field and network related to fluorescent silicon carbide for a new type of white LED in general lighting. The project resulted in recruitment of three PhD students, and about ten bachelor and master thesis students performed their diploma thesis within the topic of the network. The main project PI:s were invited to several conferences to describe the research and scientific findings. The project produced more than 30 papers, and two book chapters. The network has continued and aims to explore silicon carbide for a new photovoltaic concept by applying for research grants. It is clear that the network was made possible to realize by the approval the N-Inner(ii) project.

## Executive summary

Fluorescent SiC as material for a new type of white LED has not been previously studied. In 2006 it was indicated that SiC could be a very efficient light emitting material by doping of SiC with certain elements. However, there was no suitable growth method that could produce high quality SiC films needed for the conversion. The group at Linköping University (PI: Mikael Syväjärvi) has developed a novel growth method for thick films that produced high quality thick films. In order to be able to introduce the elements, a special SiC source material was needed. The group at Erlangen University (PI: Peter Wellmann) has previous experience in this type of doping, and developed doped PVT sources during the NORLED. The doped SiC films and sources were evaluated by KTH (PI: Margareta Linnarsson). In order to understand the luminescence from the fluorescent SiC, there is a need of optical characterization. This was realized by Denmark Technical University (PI: Haiyan Ou).

We arranged several symposia and workshops. During the project we increased the collaboration to European and International partners within the research field. There was a mobility exchange between the groups with PhD students and postdoc involved in NORLED. This is believed to be beneficial for future collaborations of the students and researchers.

## Project details

Project title	Northern Light Emitting Diode initiative
Project acronym	NORLED
Project start	Jan 2010
Project end	June 2013

	<b>Project owner</b>	<b>Project manager</b>
First name	Göran	Mikael
Last name	Hansson	Syväjärvi
Title	Professor	Associate professor
Institution	Linköping University	Linköping University
Address 1	IFM	IFM
Zip	S-58183	S-58183
City	Linköping	Linköping
Country	Sweden	Sweden
Phone	+46 13 281259	+46 13 285708
Fax	+46 13 142337	+46 13 142337
E-mail address	goh@ifm.liu.se	msy@ifm.liu.se
Web	www.ifm.liu.se/	www.liu.se/senmat

## Project partners

Coordinator: Mikael Syväjärvi

Co-coordinator: Mats Bladh (2010-2011), Haiyan Ou (2011-2013).

The project consortium is composed of three Nordic countries and Germany. Multidisciplinary (technical, social, economic) scientists are gathered together with representatives from the industry:

### SWEDEN:

Linköping University: Dr. Mikael Syväjärvi, post-doc Reza Yazdi, PhD student Remigijus Vasiliauskas, new PhD student (Material science crystal growth - FSGP development), Dr. Mats Bladh (new lighting solutions and their social tendencies), Dr. Mats Söderström (energy systems). Dr. Mats Bladh changed work position to Swedish Energy Agency during the project and was replaced by Anna Bergek.

Jönköping University:

Prof. Nils Svendenius (room lighting design)

Royal Institute of Technology:

Dr. Margareta Linnarsson (material doping evaluation)

Optoga AB:

Dr. Marcus Björkman (LED armature)

Trans Atlantic Technology AB:

MSc Johan Ekman (industrial application and production technology)

### NORWAY:

University of Oslo:

Dr. Harold Wilhite (environmental change and sustainable energy)

### DENMARK:

Technical University of Denmark:

Dr. Haiyan Ou, new PhD student (LED and optical characterization)

### GERMANY:

University of Erlangen:

Prof. Dr. Peter Wellman, PhD students MSc Michl Kaiser (fundamental SiC crystal growth and doping)

Prof. Dr. Erdmann Spiecker, one postdoc/PhD student (structural properties of doped crystals)

## Invited talks

Invited talk; "Fluorescent SiC as new material for white LEDs", Nordic Semiconductor Meeting, Fuglsøcentret, Denmark, June 19-22, 2011. Mikael Syväjärvi

Invited talk; "Growth and light properties of fluorescent SiC for white LEDs", International Conference on Silicon Carbide and Related Materials (ICSCRM), Cleveland, Ohio, USA, Sep 11-16, 2011. Mikael Syväjärvi

Invited talk; "Fluorescent SiC for energy and environment", annual Bulk Semiconductor Crystal Growth workshop (German Crystal Growth Association), Erlangen Oct 5-6, Germany, 2011. Mikael Syväjärvi

Invited Talk – German Crystal Growth Conference DKT-2012, Freiberg, 07.03.2012

Peter Wellmann

„Bulk Crystal Growth of SiC for Energy Saving Applications - Current Status and Role of Defect Reduction “

Talk – 4<sup>th</sup> European Crystal Growth Conference (ECCG4), Glasgow (UK), 18.-20.06.2012

P. Wellmann, M. Kaiser, T. Hupfer, J.W. Sun, V. Jokubavicius, P. Hens, R. Liljedahl, M. Syväjärvi, Y. Ou, H. Ou and M.K. Linnarsson: Crystal Growth and Characterization of Fluorescent SiC

Invited Talk – FhG-IISB Jahrestagung, Erlangen, 06.12.2012  
P. Wellmann, G. Neubauer, F. Roider, M. Salamon, N. Uhlmann  
"Live-Images during SiC bulk crystal growth"

Invited Talk – EU-Korea Conference on Science and Technology (EKC-2013), Brighton (UK), 24-16.07.2013  
Peter Wellmann, Georg Neubauer, Florian Roider, Michael Salamon, Norman Uhlmann  
"Towards better SiC Single Crystals by Application of in-situ 3-D Computer Tomography"

Lecture – International Summer School on Crystal Growth (ISSCG-15), Gdansk (Poland), 04.-10.08.2013  
Peter Wellmann  
"Physical Vapor Transport (PVT) Growth – with focus on SiC and brief review on AlN & GaN"

H. Ou, Y. Ou, S. Kamiyama, M. Kaiser, P. Wellmann, M. K. Linnarsson, V. Jokubavicius, R. Yakimova, and M. Syväjärvi, "Fluorescent SiC for white light-emitting diodes," Asia Communications and Photonics Conference 2012, Guangzhou, China (2012). (invited talk)

H. Ou, D. Corell, Y. Ou, P. Poulsen, C. Dam-Hansen, P. Petersen, "Spectral design flexibility of LED brings better life," Photonics West 2012, San Francisco, USA (2012). (invited talk)

## Publications

1. V. Jokubavicius, R. Liljedahl, Y. Ou, H. Ou, S. Kamiyama, R. Yakimova, and M. Syväjärvi, "Geometrical control of 3C and 6H-SiC nucleation on low off-axis substrates", Proc. European Conference on SiC and Related Materials, Oslo, Norway, Aug 29 - Sep 2, 2010, Mater. Sci. Forum 679-680 (2011) 103-106.
2. Mikael Syväjärvi, Rositza Yakimova, M. Iwaya, T. Takeuchi, I. Akasaki and Satoshi Kamiyama, "Growth and light properties of fluorescent SiC for white LEDs", invited talk at International Conference on SiC and Related Materials, Sep 11-16, 2011, Cleveland, Ohio, USA, Mater. Sci. Forum 717-720 (2012) 87-92.
3. Yiyu Ou, Valdas Jokubavicius, Chuan Liu, Rolf W. Berg, Margareta Linnarsson, Satoshi Kamiyama, Zhaoyue Lu, Rositza Yakimova, Mikael Syväjärvi, and Haiyan Ou, "Photoluminescence and Raman spectroscopy characterization of boron- and nitrogen-doped 6H silicon carbide", International Conference on SiC and Related Materials, Sep 11-16, 2011, Cleveland, Ohio, USA, Mater. Sci. Forum 717-720 (2012) 233-236.
4. Sun, J.W.; Robert, T.; Jokubavicius, V.; Juillaguet, S.; Yakimova, R.; Syväjärvi, M.; Camassel, J., "Low temperature photoluminescence signature of stacking faults in 6H-SiC epilayers grown on low angle off-axis substrates," International Conference on SiC and Related Materials, Sep 11-16, 2011, Cleveland, Ohio, USA, Mater. Sci. Forum 717-720 (2012) 407-410.
5. Valdas Jokubavicius, Michl Kaiser, Philip Hens, Peter J. Wellmann, Rickard Liljedahl, Rositza Yakimova, Mikael Syväjärvi, "Morphological and Optical Stability in Growth of Fluorescent SiC on Low Off-Axis Substrates", Materials Science Forum 740-742 (2013) 19-22.
6. Michl Kaiser, Thomas Hupfer, Valdas Jokubavicius, Saskia Schimmel, Mikael Syväjärvi, Yi Yu Ou, Hai Yan Ou, Margareta K. Linnarsson, Peter J. Wellmann, "Polycrystalline SiC as Source Material for the Growth of Fluorescent SiC Layers", Materials Science Forum 740-742 (2013) 39-42.
7. Thomas Hupfer, Philip Hens, Michl Kaiser, Valdas Jokubavicius, Mikael Syväjärvi, and Peter J. Wellmann, "Modeling of the mass transport during the homo-epitaxial growth of silicon carbide by fast sublimation epitaxy", Materials Science Forum 740-742 (2013) 52-55.

8. Saskia Schimmel, Michl Kaiser, P. Hens, V. Jokubavicius, R. Liljedahl, J. W. Sun, R. Yakimova, Y. Ou, H. Ou, M. K. Linnarsson, P. Wellmann and M. Syväjärvi, "Step-flow growth of fluorescent 4H-SiC layers on 4 degree off-axis substrates", *Materials Science Forum* 740-742 (2013) 185-188.
9. Kanaparin Ariyawong, Valdas Jokubavicius, Rickard Liljedahl, and Mikael Syväjärvi, "Step instability in sublimation epitaxy on low off-axis 6H-SiC", *Materials Science Forum* 740-742 (2013) 201-204.
10. Margareta K. Linnarsson, Michl Kaiser, Rickard Liljedahl, Valdas Jokubavicius, Yi Yu Ou, Peter J. Wellmann, Hai Yan Ou, Mikael Syväjärvi, "Lateral Boron Distribution in Polycrystalline SiC Source Materials", *Materials Science Forum* 740-742 (2013) 397-400.
11. G. Neubauer, F. Roider, M. Salamon, N. Uhlmann, P.J. Wellmann; Application of 3D X-Ray Computer Tomography for the In-Situ Visualization of the SiC Crystal Growth Interface during PVT Bulk Growth; *Mater.Sci.Forum* 740-742, p.27 (2013).
12. Jian Wu Sun, Satoshi Kamiyama, Rositza Yakimova, Mikael Syväjärvi, "Effect of Surface and Interface Recombination on Carrier Lifetime in 6H-SiC Layers", *Materials Science Forum* 740-742 (2013) 490-493.
13. Y. Ou, V. Jokubavicius, M. Kaiser, P. Wellmann, M. K. Linnarsson, R. Yakimova, M. Syväjärvi, and H. Ou., "Fabrication of broadband antireflective sub-wavelength structures on fluorescent SiC", *Materials Science Forum* 740-742 (2013) 1024-1027.
14. Vytautas Grivickas, Karolis Gulbinas, Valdas Jokubavicius, Jian Wu Sun, Yiyu Ou, Haiyan Ou, Margareta Linnarsson, Mikael Syväjärvi, Satoshi Kamiyama, "Carrier Lifetimes in Fluorescent 6H-SiC for LEDs Application", *Lithuanian National Physics Conference*, Oct 6-7, 2011, Vilnius, Lithuania.
15. Yiyu Ou, Valdas Jokubavicius, Satoshi Kamiyama, Chuan Liu, Rolf W. Berg, Margareta Linnarsson, Rositza Yakimova, Mikael Syväjärvi, and Haiyan Ou, "Donor-acceptor-pair emission characterization in N-B doped fluorescent SiC" *Optical Materials Express* 1 (2011) 1439-1446.
16. J.W. Sun, V. Khranovskyy, M. Mexis, M. Eriksson, M. Syväjärvi, I. Tsiaoussis, G.R. Yazdi, H. Peyre, S. Juillaguet, J. Camassel, P.O. Holtz, P. Bergman, L. Hultman, R. Yakimova, "Comparative micro-photoluminescence investigation of ZnO hexagonal nanopillars and the seeding layer grown on 4H-SiC", *J. Luminescence* 132 (2012) 122-127.
17. M. Asghar, F. Iqbal, S.M. Faraz, V. Jokubavicius, Q. Wahab and M. Syväjärvi, "Study of deep level defects in doped and semi-insulating n-6H-SiC epilayers grown by sublimation method", *Physica B: Condensed Matter* 407 (2012) 3038-3040.
18. M. Asghar, F. Iqbal, S.M. Faraz, V. Jokubavicius, Q. Wahab and M. Syväjärvi, "Characterization of deep level defects in sublimation grown p-type 6H-SiC epilayers by deep level transient spectroscopy", *Physica B: Condensed Matter* 407 (2012) 3041-3043.
19. Yiyu Ou, Valdas Jokubavicius, Philip Hens, Michl Kaiser, Peter Wellmann, Rositza Yakimova, Mikael Syväjärvi, and Haiyan Ou: "Broadband and omnidirectional light harvesting enhancement of fluorescent SiC", *Optics Express* 20 (2012) 7575-7579.
20. Yiyu Ou, Valdas Jokubavicius, Rositza Yakimova, Mikael Syväjärvi, and Haiyan Ou: "Omnidirectional luminescence enhancement of fluorescent SiC via pseudoperiodic antireflective subwavelength structures", *Optics Letters* 18 (2012) 3816-3818.
21. V. Jokubavicius, P. Hens, R. Liljedahl, J. W. Sun, M. Kaiser, P. Wellmann, S. Sano, R. Yakimova, S. Kamiyama and M. Syväjärvi, "Effects of Source Material on Epitaxial Growth of Fluorescent SiC", *Thin Solid Films* 522 (2012) 7-10.
22. Satoshi Kamiyama, Motoaki Iwaya, Tetsuya Takeuchi, Isamu Akasaki, Rositza Yakimova, Mikael Syväjärvi, "White light-emitting diode based on fluorescent SiC", *Thin Solid Films* 522 (2012) 23-25.

23. J.W. Sun, V. Jokubavicius, R. Liljedahl, R. Yakimova, S. Juillaguet, J. Camassel, S. Kamiyama, and M. Syväjärvi, "Room temperature luminescence properties of fluorescent SiC as white light emitting diode medium", *Thin Solid Films* 522 (2012) 33-35.
24. M Syväjärvi, J Müller, JW Sun, V Grivickas, Y Ou, V Jokubavicius, P Hens, M Kaisr, K Ariyawong, K Gulbinas, P Hens, R Liljedahl, M K Linnarsson, S Kamiyama, P Wellmann, E Spiecker, and H Ou: "Fluorescent SiC as new material for white LEDs", *Physica Scripta T148* (2012) 14002.
25. Y Ou, V Jokubavicius, M K Linnarsson, R. Yakimova, M Syväjärvi, and H Ou: "Characterization of donor-acceptor-pair emission in fluorescent 6H-SiC", *Physica Scripta T148* (2012) 14003.
26. J W Sun, S Kamiyama, V Jokubavicius, H Peyre, R Yakimova, S Juillaguet and M Syväjärvi, "Fluorescent silicon carbide as an ultraviolet-to-visible light converter by control of donor to acceptor recombinations" *J. Phys. D: Appl. Phys.* 45 (2012) 235107/1-6.
27. Mikael Syväjärvi, "Perspectives of fluorescent and cubic silicon carbide", *Adv. Mat. Lett.* 3 (2012) 175
28. J. W. Sun, T. Robert, A. Andreadou, A. Mantzari, V. Jokubavicius, R. Yakimova, J. Camassel, S. Juillaguet, E. K. Polychroniadis, and M. Syväjärvi, "Shockley-Frank stacking faults in 6H-SiC", *J. Appl. Phys.* 111 (2012) 113527.
29. Zhu, XL, Ou, YY, Jokubavicius, V, Syväjärvi, M, Hansen, O, Ou, HY, Mortensen, NA, and Xiao, SS, "Broadband light-extraction enhanced by arrays of whispering gallery resonators", *Appl. Phys. Lett.* 101 (2012) 241108.
30. Bergek, A. & Onufrey, K. (2013): Is one path enough? Multiple paths and path interaction as an extension of path dependency theory, under review by *Industrial and Corporate Change* (major revision; revised manuscript submitted).
31. Onufrey, K. & Bergek, A. (2013): Self-reinforcing mechanisms and multi-path dynamics: insights from applying the Technological Innovation Systems (TIS) perspective, paper presented at the *R&D Management Conference 2013*, Manchester, 26-28 June 2013.
32. Bergek, A. & Onufrey, K. (2012): Path dependency in industries with multiple technological trajectories, paper presented at the *2012 International Schumpeter Society Conference*, Brisbane, 2-5 July 2012.
33. I. Shtepliuk, V. Khranovskyy, G. Lashkarev, V. Khomyak, V. Lazorenko, A. Ievtushenko, M. Syväjärvi, V. Jokubavicius, and R. Yakimova, "Electrical properties of n-Zn<sub>0.94</sub>Cd<sub>0.06</sub>O/p-SiC heterostructures", *Solid State Electronics* 81 (2013) 72-77.
34. M. Bladh and M. Syväjärvi (Eds): "New Lighting—New LEDs: Aspects on light emitting diodes from social and material science perspectives", Linköping University Electronic Press (2010), ISBN 978-91-7393-270-7.

## Organised symposia and workshops

Workshop on Crystal Growth of Semiconductors (German Crystal Growth Association DGKK), Crystal Growth and Characterization of bulk semiconductor crystals", October 5-6, 2011 (German Crystal Growth Association DGKK), Germany

Symposium in the first Bilateral Energy Conference at the E-MRS Spring Meeting, "Engineering of wide bandgap semiconductor materials for energy saving", May 9-13, 2011, European Materials Research Conference (E-MRS) France

Organization of the One-Day-PV-Symposium in the first Bilateral Energy Conference at the E-MRS Spring Meeting, "From Semiconductors to New Energy – the PV Value added Chain", May 11, 2011, European Materials Research Conference (E-MRS) France

Symposium in conference, "Alternative approaches of SiC and related wide bandgap materials in light emitting and solar cell applications", E-MRS 2013 Spring meeting, May 27-31, 2013 Strasbourg, France.

Meijo-DTU workshop on research and development of light-emitting diodes, 15<sup>th</sup> of March, 2013.

## **Other issues**

Haiyan Ou received the Strategic Research Award 2013 from Danish Ministry of Science, Innovation and Higher Education. Motivation: "Haiyan Ou has developed a way of making LED lighting even more energy efficient and more pleasant to look at. She has achieved this with a nanostructuring method which causes a reflection reduction from SiC from 20 % down to 1.6 %." Haiyan Ou founded a spin off company Light Extraction APS that commercializes the nanostructuring process.

The project is summarized by the following chapter.

## ADVANCES IN WIDE BANDGAP SiC FOR OPTOELECTRONICS

Haiyan Ou<sup>1</sup>, Yiyu Ou<sup>1,2</sup>, Aikaterini Argyraki<sup>1</sup>, Saskia Schimmel<sup>3</sup>, Michl Kaiser<sup>3</sup>, Peter Wellmann<sup>3</sup>, Margareta K. Linnarsson<sup>4</sup>, Valdas Jokubavicius<sup>5</sup>, Jianwu Sun<sup>5,6</sup>, Rickard Liljedahl<sup>5</sup>, Mikael Syväjärvi<sup>5</sup>

<sup>1</sup> *Department of Photonics Engineering, Technical University of Denmark, DK-2800, Lyngby, Denmark*

<sup>2</sup> *Presently with Light extraction ApS, DK-2800, Denmark*

<sup>3</sup> *Materials of Electronics Energy Technology, University of Erlangen-Nuremberg, D-91058, Erlangen, Germany*

<sup>4</sup> *School of Information and Communication Technology, KTH Royal Institute of Technology, SE-16440, Kista, Sweden*

<sup>5</sup> *Department of Physics, Chemistry and Biology, Linköping University, SE-58183, Linköping, Sweden*

<sup>6</sup> *Presently with IMEC, Kapeldreef 75, B-3001 Leuven, Belgium*

### Abstract

Silicon carbide (SiC) has played a key role in power electronics thanks to its unique physical properties like wide bandgap, high breakdown field etc. During the past decade, SiC is also becoming more and more active in optoelectronics thanks to the progress in material growth and nanofabrication. This paper will review the advances in fluorescent SiC for white light-emitting diodes, covering the poly-crystalline fluorescent SiC source material growth, single crystalline epitaxy growth of fluorescent SiC, and nanofabrication of SiC to enhance the extraction efficiency for fluorescent SiC based white LEDs.

### 1. Introduction

Silicon carbide (SiC) is the only group IV compound semiconductor, and it has more than 200 polytypes. Among them the most commonly used are 4H, 6H, 3C and 15R. The wide bandgap makes SiC a very attractive semiconductor to make devices for applications in high power, high frequency and high temperature environment.

In addition to the traditional applications, SiC has been emerging as a promising material for light-emitting diodes (LED) since Satoshi Kamiyama in 2006 found that nitrogen (N) and boron (B) co-doped SiC has very high donor-acceptor pair (DAP) emission efficiency [1].

LED light sources are deemed to be the future market leader thanks to their energy saving and long lifetime, compared to conventional incandescent lamps and fluorescent tubes. Currently, most white LED light sources available in the market are made by mixture of blue color from a blue GaN LED and yellow color emitted from the phosphor excited by the blue LED, as shown in Fig.1 (a). However, there is always a tradeoff between high lumen efficiency and high color rendering index (CRI) for this type of light source. The phosphor degrades much faster than the blue LED chip, so the white light turns blue over time. Moreover, phosphor contains rare earth elements, which could be a price bottleneck considering the huge market in future. In order to overcome these limitations and explore the full potential of the LED light source, a new type white LED light source based on fluorescent SiC (f-SiC), shown in Fig.1 (b), has been

proposed. Compared to the phosphor based white LED light source, this f-SiC based white light source has a number of advantages: a) it could have both high efficiency and high color rendering index, opposite to the trade-off observed for phosphor based white LED light sources; b) it has even longer lifetime due to the monolithic semiconductor structure; c) it has simpler thermal management because SiC is a very good thermal conductor; and d) it doesn't contain rare-earth elements.

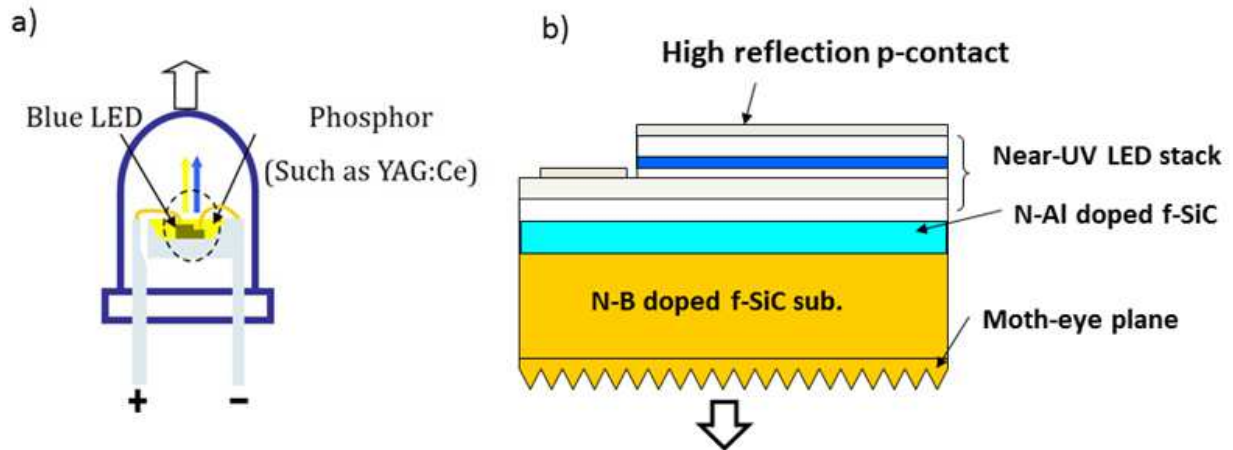


*Fig.1 Schematic drawing of (a) traditional phosphor based white LEDs. The white color is mixed with blue color from an LED chip and yellow color from the phosphor excited by the blue and (b) the new fluorescent SiC based white LED.*

As shown in Fig. 1(b), the f-SiC based white LED light source uses f-SiC as a substrate as well as a wavelength converter. It consists of one layer of 200  $\mu\text{m}$  thick N and B co-doped SiC and one layer of 50  $\mu\text{m}$  thick N and aluminium (Al) co-doped SiC. A near ultraviolet (NUV) diode is grown on top of the N and Al co-doped SiC. A mirror is formed on top of the NUV diode and divert all the light to exit from the f-SiC substrate. Silicon carbide has a refractive index of 2.65 at 590 nm [2], causing most of the emitted light from f-SiC to be totally reflected into the device. In order to enhance the light extraction efficiency, as shown in Fig. 1(b), moth-eye nanostructures are implemented at the exit surface of the f-SiC to increase the emission efficiency in the whole visible spectral range.

The operational mechanism of the f-SiC based white LED is illustrated in Fig. 2

The high energy NUV photons emitted from the NUV LED excite electrons from the top of the valence band to the bottom of the conduction band. The free electrons in the conduction band and the free holes left in the valence band will occupy the donor level (N) and acceptor level (Al and B), respectively, obeying the Fermi-Dirac distribution. Then, the electrons on the donor level will recombine with the holes on the acceptor level and emit a low energy photon. The N and Al donor-acceptor-pair (DAP) recombination emits blue light with peak wavelength around 480 nm and N and B DAP emits yellow light with peak wavelength around 590 nm since B is a much deeper acceptor in SiC with respect to the Al. The mixture of the broadband blue light and broadband yellow light makes white light with high CRI.

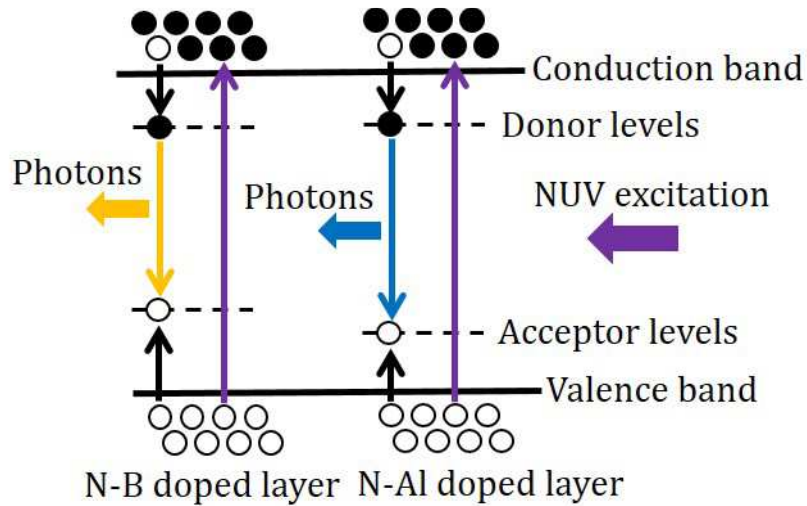


Fig. 2 Schematic drawing of the operational mechanism of the f-SiC based white LED light source

The f-SiC based white LED light source is an innovative achievement for SiC in optoelectronic devices. In order to accomplish such a new device concept, the development of the material is crucial. In this paper, poly-crystalline f-SiC source material is firstly optimized to grow by physical vapor transport (PVT) after comparing sintering, chemical vapor deposition (CVD) and PVT methods, described in section 2. Then the source material (poly-crystalline SiC) is used for the growth of high quality single crystalline SiC by fast sublimation growth process (FSGP), described in section 3. Section 4 presents the optical characterization of the grown epilayers in terms of photoluminescence and Raman spectroscopy to feedback the optimal growth conditions. In order to enhance the extraction efficiency, a couple of different nanostructuring methods were applied on the f-SiC surface and described in section 5. Both periodic and non-periodic structures have been demonstrated and effectively increased the emission efficiency. Section 6 summaries the advances of f-SiC in LED application and gives future perspectives in optoelectronic applications.

## 2. Poly-crystalline fluorescent SiC growth

For the epitaxial growth of high quality fluorescent SiC layers by the FSGP process, the application of a proper solid SiC source material is crucial. In principle, three approaches have been followed so far to produce the desired source material: (a) sintering of SiC powder, (b) chemical vapor deposition (CVD) of microcrystalline SiC and (c) bulk growth of polycrystalline SiC boules by the so called physical vapor transport (PVT) technique. Application of sintered SiC ceramic as source (Fig. 3(a)) does not lead to mirror like epitaxial layers. In addition, inclusions of secondary phases, most likely carbon related defects, are found in the grown epitaxial SiC material. This type of sintered source easily graphitizes during the SiC epitaxy. In the case of the CVD SiC source material (Fig. 3(b)) inclusions of 3C-SiC in the 6H-SiC epitaxial layers are found, which are related to the source material used in the epitaxial growth process. A main challenge with this source is the uniform doping introduction. Due to the small size of the inclusions it is concluded that they originate from mass transport between source and seed. Finally, in the case of the PVT growth SiC source (Fig. 3(c)) the lowest defect density and, hence, best f-SiC layer properties with basically no inclusions are found. In the following this vapor grown source material will be reviewed in detail.

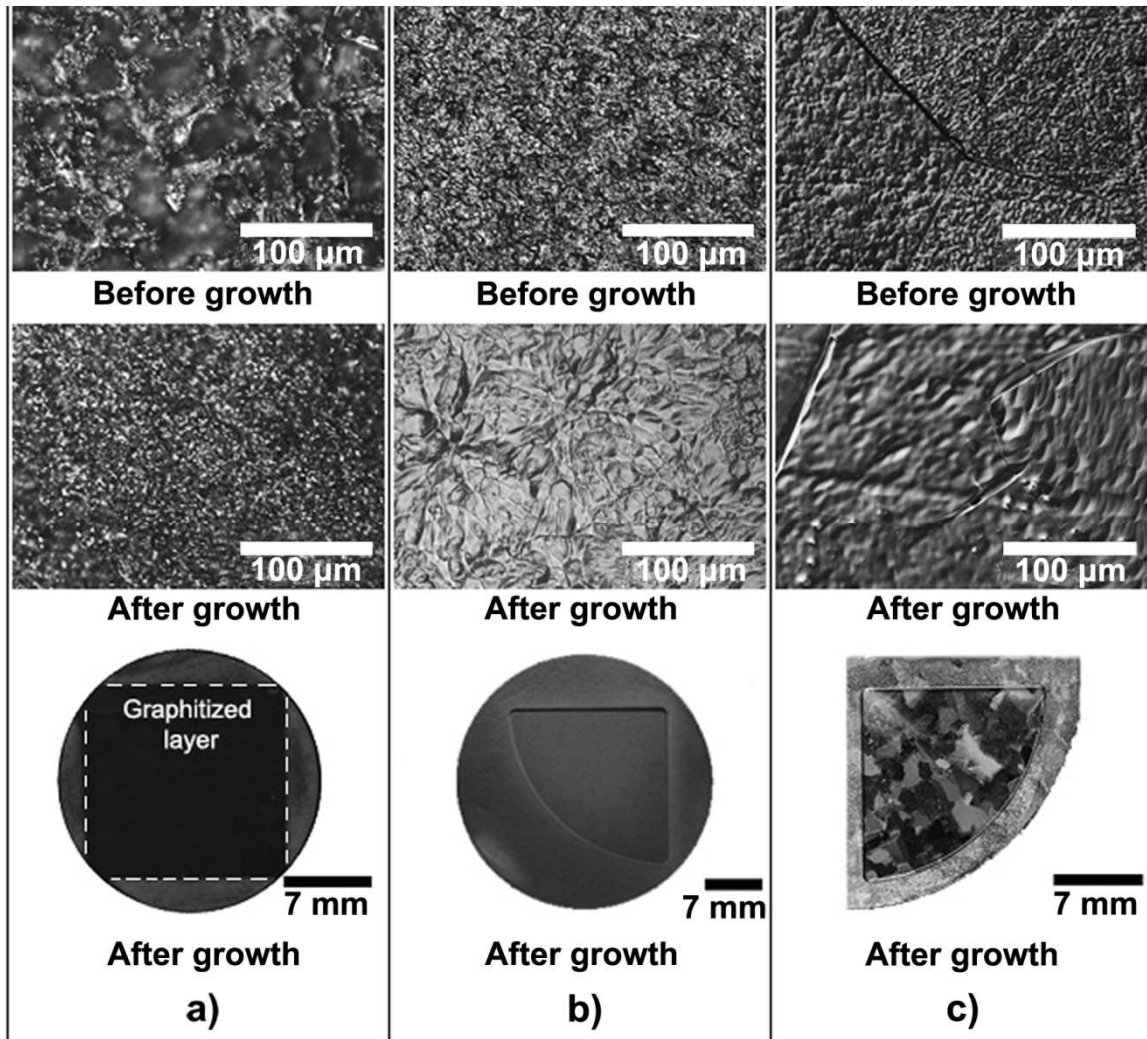


Fig.3 Comparison of three SiC source materials for application during FSGP: (a) sintered poly-crystalline SiC ceramics, (b) CVD grown micro-crystalline SiC source and (c) PVT grown poly-crystalline SiC material. The best layer properties are found in the case of the PVT grown source materials. (Fig. from [3])

## 2.1 PVT growth process, doping of poly-SiC and wafering process

### 2.1.1 Growth Process Principle

Growth of poly SiC source material is carried out by the state-of-the-art physical vapor transport (PVT) method (see Fig. 4(a)). SiC powder is placed at the bottom of the graphite crucible. As self-seeding substrate a graphite plate is used which is attached to the top of the crucible. Inducting heating is performed in a way that a temperature difference of approximately 50°C is established between the top of the SiC powder source and the poly SiC growth interface. Typical growth rates lie in the range of 200 μm/h and 1000 μm/h and depend on the absolute temperature between 2010°C and 2300°C at the crucible top, as well as on the ambient noble gas pressure between 10 mbar and 40 mbar.

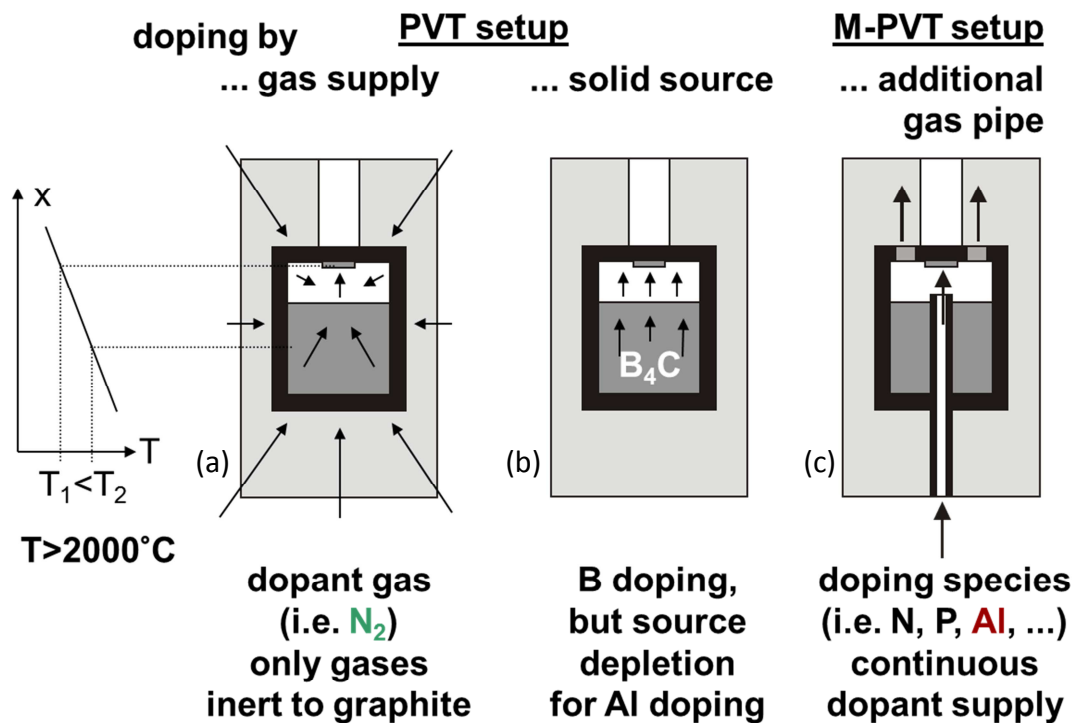


Fig. 4 Sketch of the PVT growth reactor interior for the preparation of doped poly-SiC boules.

### 2.1.2 Doping of SiC by N, B and Al

As dopants nitrogen from the 5<sup>th</sup> main group was used as donor, while aluminum and boron from the 3<sup>rd</sup> main group act as acceptors in SiC. The supply of nitrogen can be applied by addition of a  $N_2$  gas stream to the ambient inert gas stream (Fig. 4(a)). Due to the chemical inertness of nitrogen and carbon, the dopant gas diffuses through the partially porous graphite parts of the crucible and the surrounding isolation. In the case of the acceptor dopants aluminum and boron the latter procedure fails. Boron may be supplied by addition of boron, in particular boron carbide ( $B_4C$ ) to the source material (Fig. 4(b)). The dopant transfer from source to growing crystal, as well as incorporation into SiC can be well controlled by the  $B_4C$  mass fraction directly added to the SiC source material [4]. In the case of aluminum, however, the dopant supply is more complex. In this case, a too high initial aluminum partial pressure is observed if the dopant is directly added to the SiC source material. In order to suppress the large axial dopant concentration variation in the final SiC crystal, a slightly varied technique, the so called Modified-PVT (M-PVT) method, is applied [5, 6] (Fig. 4(c)). In the M-PVT setup an aluminum source ( $Al_4C_3$ ) is placed at a lowered temperature and, hence, smaller aluminum vapor pressure in the near vicinity of the PVT crucible. Via a feeding gas pipe the dopant is continuously added to the growth chamber exhibiting a constant dopant flow during the growth process.

### 2.1.3 Wafering

Subsequent to growth the poly-SiC boules are grinded down to a proper diameter of typically 50 mm. Wafering is carried out by a diamond inside hole saw. Wafer thickness lies between 500  $\mu m$  and 1 mm. For the application as source material during FSGP a removal of the sawing damage by a lapping or rough polishing step is necessary.

## 2.2 Structural properties of poly-SiC wafers

During polycrystalline growth of SiC a pronounced grain growth is observed which is attributed to a strong grain selection process [7]. Figure 5 shows optical scanning images of three poly SiC wafers from the same boule directly (a) after nucleation, (b) after 10h and (c) after 20h of growth time. As substrate plate is statically pressed, highly purified graphite was used. The polytypes differ from 4H-SiC, 6H-SiC and 15R-SiC. No 3C-SiC was found which may be related to the high growth temperature above 2100°C. Although no precise and well defined grain orientation is observed by x-ray Laue pattern analysis (40kV, 30mA, 5min), most grains exhibit a trend towards (0001) orientation with inclination variation between 0° and 30°. Between the grains no obvious preferential alignment, i.e. formation of particular grain boundaries, was detected so far. Noteworthy is that 15R-SiC grains usually exhibit off orientation towards (0001) of more than 15°. From KOH defect etching analysis it is concluded that more than 90% of the larger grains (Fig. 5(b) and 5(c)) show C-face polarity. Pretreatment of the statically pressed graphite nucleation plate surface by coating with pyrolytic graphite showed an impact on the variation of grain orientation and grain selection process. Compared to the partially porous isostatic pressed graphite with mainly random grain orientation, the pyrolytic coating exhibits no open porosity and a [001]-texture and slightly reduced surface roughness. As main result, a SiC grain size in the 10 mm range has been observed, but further studies are necessary to quantify these new findings (Fig. 6)[8]. The weak impact of the SiC grain polytype and orientation on the growth rate during FSGP will be discussed in section 2.4.

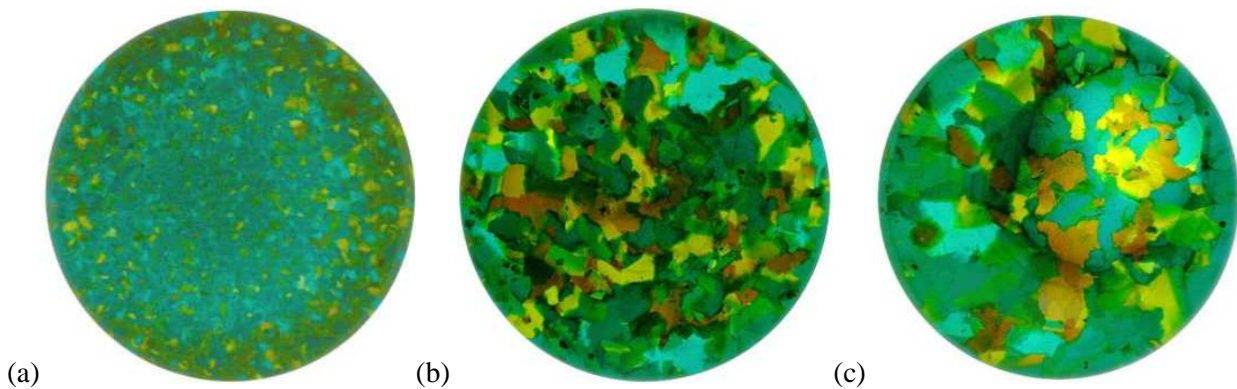


Fig.5 White light absorption scans of a series of three 50 mm poly SiC wafers from boule: (a) directly after nucleation, (b) after 10h and (c) after 20h of growth time (Fig. from [7]).

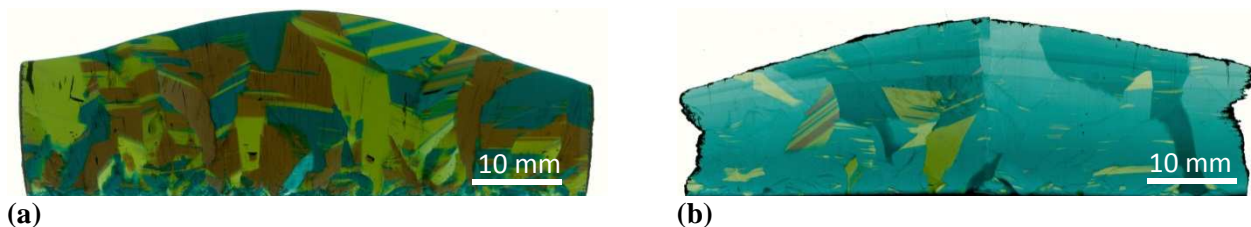


Fig.6 Cross section of two poly SiC crystals grown on isostatic graphite at 2250°C (a) and on pyrolytic graphite at 2350°C (b). The diameter of the cross section of the boules of >60 mm is shown before grinding down to the standard size of 50 mm (Fig. from [8]).

### 2.3 Electrical properties of poly-SiC wafers

The N, B and Al doping concentration of the poly SiC source is set by (i) the amount of dopant supply, (ii) growth rate and (iii) growth kinetic related boundary conditions (e.g. C/Si ratio of the SiC vapor) which are related to the growth parameters like temperature field and inert gas pressure. Amount of dopant supply is mainly given by intentional feeding; however, residual doping of the powder SiC source prior PVT growth and contamination from the crucible material also has to be considered. In the case of B doping with target values in the mid  $10^{18}\text{cm}^{-3}$  (chemical concentration) the amount of addition to the SiC source powder is the dominant factor.

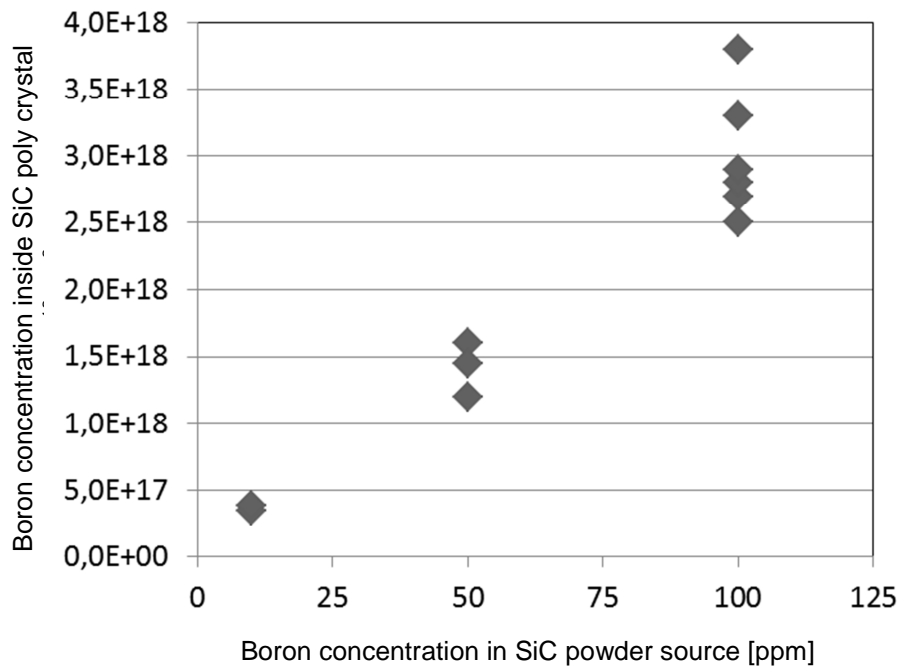


Fig. 7 Plot of boron incorporation into poly SiC during PVT growth.

Fig. 7 shows the experimental evaluation between addition of boron as  $\text{B}_4\text{C}$  to the SiC powder source and chemical composition inside the poly-SiC crystal for a number of wafers. The dopant transfer from source to seed crystal is well defined by the amount of supply and growth parameters (temperature and pressure). Doping variations of ca. 25% to 50% are mainly related to kinetic dopant incorporation effects due to varying crystallographic orientations of the grains in the range of tilt angles around between  $0^\circ$  and  $30^\circ$  towards (0001) orientation (see section 2.2). While local doping may vary around the mentioned 25 to 50%, the medium values can be set around 10% to 15% by proper and reproducible setting of the growth process parameters.

## 2.4 Impact of structural source properties on growth rate during FSGP

In order to study the impact of the structural properties of the poly-SiC source wafers on the FSGP growth rate, special experiments with masking techniques were carried out. During FSGP a graphite mask was placed between source and seed to select certain SiC grains from the source material and to follow the impact of polytype and grain orientation on the epitaxial layer thickness, as shown in Fig. 8.

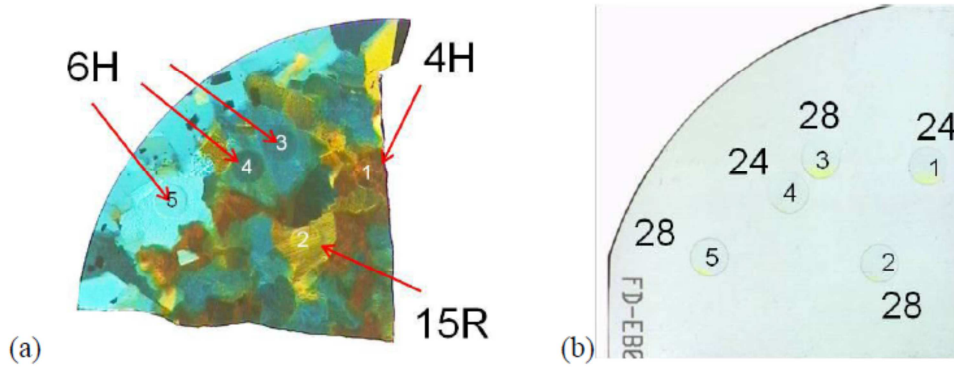


Fig. 8 Optical Image of (a) poly-SiC source material and (b) grown 6H-SiC FSGP layer. The circles with numbers 1 to 5 indicate 5 growth areas selected by graphite mask.

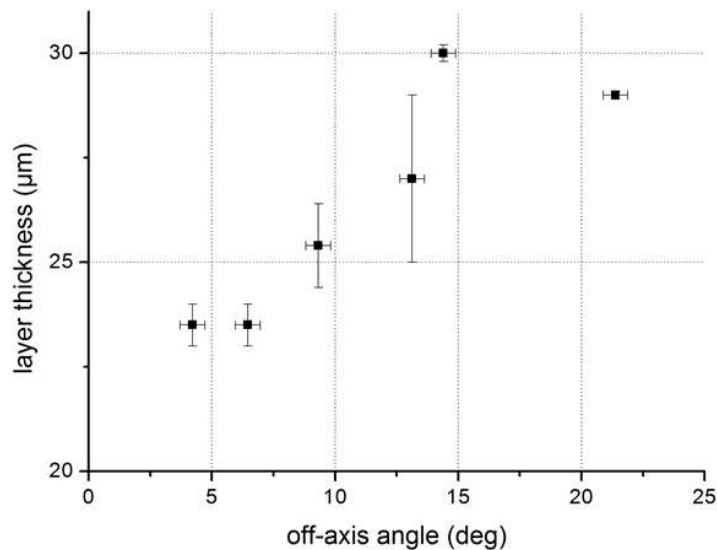


Fig. 9 Impact of off-axis angle orientation of Poly-SiC source materials grains on growth rate / layer thickness during FSGP epitaxy. (Figure after [7])

Table 1: Summary of grain orientation (off-axis angle) and polytype of the source material on layer thickness during FSGP epitaxy. (Table after [7])

Grain	Polytype	average layer thickness [ $\mu\text{m}$ ]	off-orientation [deg]
1	4H	23.5	4.2 +/- 0.5
1	4H	23.5	6.5 +/- 0.5
2	15R	29	21.4 +/- 0.5
3	6H	27	13.1 +/- 0.5
4	6H	25.5	9.3 +/- 0.5
5	6H	30	14.4 +/- 0.5

The graphical analysis of the limited data exhibits a clear correlation between of axis orientation (tilt of the grain off orientation towards (0001)) and epitaxial layer thickness. With increasing off orientation the growth rate and layer thickness increases. Projected to a 2 inch epitaxial process local thickness variations of +/- 10% have to be considered. The data in Fig. 9 and Table 1 also include polytype variations. However, the effect of grain polytype on FSGP growth rate is covered by the dominating grain orientation effect. It is estimated from the data in Table 1 that the variation of grain polytype impacts layer thickness is below 5%. Depending on the vapor pressure during FSGP the local influence is believed to be lowered in case of greater inert gas pressures [9].

### 3. Single-crystalline fluorescent SiC epitaxial growth

#### 3.1 Homoepitaxial growth aspects of SiC

Historically, most studies of SiC epitaxial layers have been using the chemical vapor deposition (CVD) method. Initially, heteroepitaxial growth was performed on silicon substrates, and epitaxial layers of 3C-SiC were studied. In the 1990's, 6H-SiC substrates became commercially available from PVT growth, and allowed more intense homoepitaxial growth studies. The first wafers had an on-axis orientation, and this caused a competition between the homoepitaxial 6H-SiC growth and 3C-SiC inclusions. In order to reduce these inclusions, the surface was prepared with a slight off-axis orientation and the homoepitaxial growth could be fully realized without inclusions of other polytypes. The standard off-axis angle for the 6H-SiC became 3.5 degrees in the [11-20] direction. Later on, 4H-SiC substrates became available from the bulk growth. It was found that a 3.5 degree off-orientation was not sufficient to maintain the polytype stability in 4H-SiC, and inclusions of 3C-SiC appeared in the epitaxial growth. The standard off-orientation was modified to have an 8 degree off-axis for homoepitaxial growth in 4H-SiC.

In growth of nitride layers, the on-axis surface has been preferred. An off-axis surface could result in compositional changes of the nitride layers, and a large off-axis is therefore very challenging to use. In the growth of fluorescent SiC homoepitaxial layers, the low off-axis growth was implemented [101-20]. This off-axis was in the range from 0.8 to 1.4 degrees. Both SiC and nitride growth may then be adapted to handle polytype inclusions and compositional effects with some modifications of growth conditions.

For the fluorescent SiC layer, a voluminous layer is needed. The CVD method has shown to be promising for pure layers suitable for transistor applications, while a high growth rate has been challenging, and thick layers are hard to produce. The growth rate may be some tens of  $\mu\text{m/hr}$ , but typically less than 10  $\mu\text{m/hr}$  to maintain a reasonable surface morphology. The natural habit for SiC is sublimation. The use of close spacing for growing epitaxial layers has been introduced and applied for GaAs, Ge, GaP, and CdS [12]. The sublimation sandwich configuration that was applied for SiC [13-14] is a process that may be applied for

growth of thick layers. This method was further elaborated in several studies by Kyoto Institute of Technology and Linköping University [15-17]. In particular, the ability to demonstrate the combination of fast sublimation growth process and structural quality makes the methods suitable for growth of fluorescent SiC [18].

In comparison, boule growth is typically applied by PVT growth at high temperature like 2300-2500°C. The corresponding growth rates are several hundreds of micrometer per hour. The growth is controlled by an ambient pressure of argon or nitrogen in the 5-50 mbar range. The typical source to seed distance is 5-30 mm, and the source is a SiC powder. The Fast Sublimation Growth Process (FSGP) [18] is a modification of the PVT growth. The growth temperature is reduced to less than 2000°C and use of vacuum or low pressure at which the surface kinetics is determining the growth rates rather than diffusion of species in the ambient. By a shorter distance between source and substrate to about 1 mm, the growth is epitaxial while the high growth rate and possibility of growing thick layers is maintained. Typical growth rates and growth temperatures are 50-300  $\mu\text{m/hr}$  at 1750-1900°C.

### 3.2 Polytype stability and luminescence in fluorescent SiC layers

In general, the growth on off-oriented SiC substrates proceeds via step-flow growth [19]. In this mode, steps are created when the SiC is heated and at the initial stage of growth. Atoms on the surface are diffusing to the kink site of the step, and the polytype of the substrate is reproduced since the crystal arrangement is unique at the kink. With increasing layer thickness, there are on-axis regions that are created. These in principle are of two types. The first one is at the edge of the substrate, where an on-axis region is created in the upstep direction when the layers become very thick. The second is given by the terraces of the steps. When steps merge and give rise to step-bunching [20-21], the steps are increasing with their step height, but also in the width of the step. On the terrace, the on-axis region becomes larger. At some point, the atoms do not have time to diffuse to the step edge, and may form a growth center on the terrace. This might form as a 3C-SiC structure. Moreover, we have found that in the fluorescent 6H-SiC grown on the 1.4 degree off-axis substrate, the transition region from 6H-SiC to the 3C-SiC part also shows the presence of a series of stacking faults by the low temperature photoluminescence (LTPL) and high resolution transmission electron microscopy studies [26]. These stacking faults can trap the photo-excited carriers and thus reduce the luminescence efficiency.



*Fig. 10 Surfaces of samples grown on quarter of 2 inch wafer with 50 ppm B doping: (a) overall figure, a 3C area is marked by a ring; (b) optical microscopy image, scale 10  $\mu\text{m}$ ; (c) SEM image, scale 4  $\mu\text{m}$ .*

In general, the morphology of epitaxial layers grown by sublimation epitaxy shows a smooth surface without any traces of steps that can be observed in the optical microscope even when using Nomarski interference contrast mode, Fig. 10. In comparison, the use of PVT source in growth of fluorescent silicon carbide layers gives rise to observable steps. In addition, the steps are quite straight in nominally undoped growth while some curvatures are observed in the doped growth. Typically in silicon carbide epitaxial and crystal growth,

step bunching might appear when the C/Si ratio is high [22]. However, there is no graphitization of the PVT source that was used for the growth of the layers. In the sublimation epitaxy, if graphitization occurs, the source graphitizes first and then the epitaxial layer. The reason for faintly curved steps is not fully clear, but one could consider the influence of impurities on the step trains that gives rise to an instability. For example, it was observed that there is step bunching in PVT growth at high nitrogen concentration [23]. In that work, upon nitrogen doping, the regular step trains on 6H-SiC(0001) become unstable. The equidistant step trains are transformed into meandering macrosteps, explained by the nitrogen adsorption on the growing crystal surface.

The source material for a warm white LED contains only nitrogen and boron. This is produced by a mixture of boron carbide in the SiC source and having various nitrogen flows during the PVT growth. Thereby there will be both nitrogen and boron in the source. Boron is typically transferred at high ratio, around 80% is transferred from the polycrystalline source to the growing epilayer. In comparison, nitrogen transfer is substantially less, like 10%.

In a simple PL set-up, one can distinguish the influence of high nitrogen content in the source. A series of PVT sources with different boron content in the SiC powder were grown at high nitrogen flow. The nitrogen seems to overcompensate the boron in all cases. However, the luminescence with different boron content is very scattered using an initial nitrogen pressure in the FSGP, shown in Fig. 11. The initial ambient nitrogen pressure is set by closing of valves and there is a background ambient in contrast to the case when there is a constant flow of nitrogen. In the case when there is a high content of nitrogen in the source, the initial ambient nitrogen pressure is very low. Therefore it is consequently also sensitive to changes in setting of initial pressure.

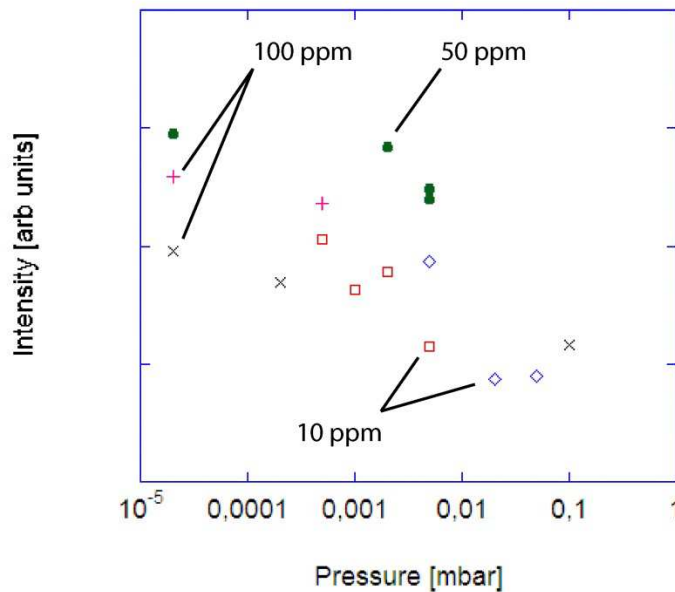


Fig. 11 Photoluminescence intensity change in a simple PL box with sources produced with 10, 50 and 100 ppm of boron at 8 sccm  $N_2$  flow at different initial levels of nitrogen ambient pressure.

It seems that in source with high nitrogen content, there is no need to add nitrogen from the ambient. Therefore we have applied a static approach. In this, the system is pumped to a base pressure around  $10^{-5}$  mbar. Then the valve is closed and heating starts. By this there is very low sensitivity to setting of ambient pressure since this is not operator dependent. We have applied three different conditions for such static vacuum approach. The valve to the pump was closed at three temperatures: room temperature (static RT), after heating to  $1000^\circ\text{C}$  (static 1000), and heating to  $1250^\circ\text{C}$  (static 1250). With this approach, the increase in

luminescence with different concentrations of boron in the source, that has a high nitrogen content, shows a clear positive trend, Fig. 12.

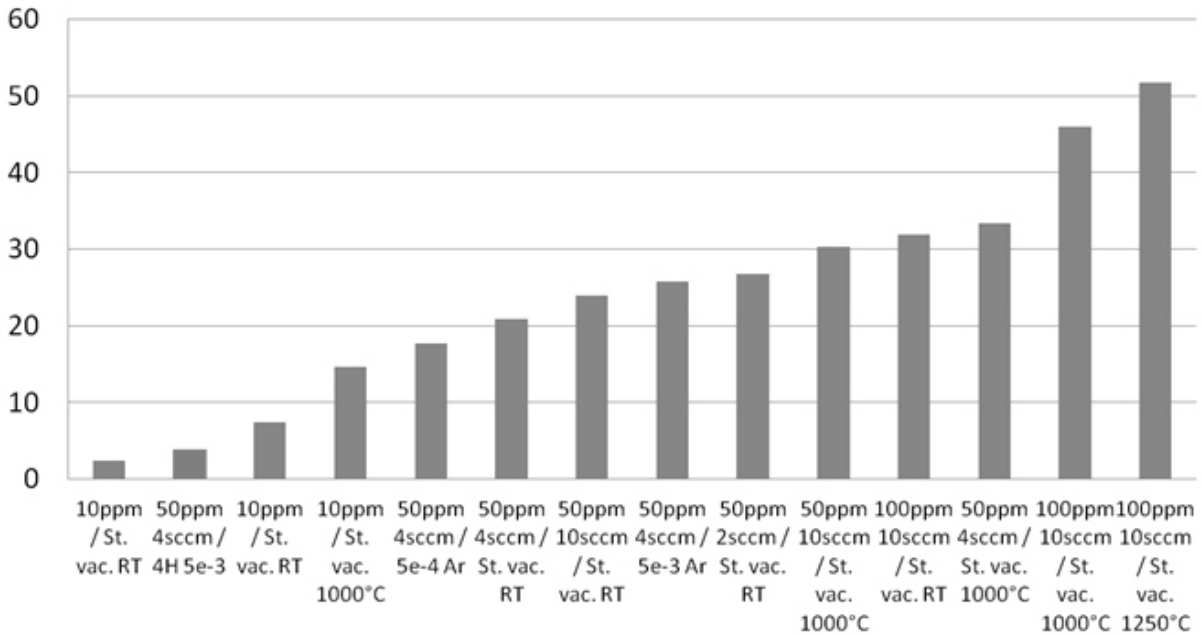


Fig. 12 Luminescence intensity with increasing boron doping and at which temperature the valve to pump is closed.

Indeed, there is clear luminescence from the grown layers, Fig. 13. It has been shown that in sublimation epitaxy, there is a structural improvement from the substrate to the epilayer [24]. In FSGP growth of fluorescent layers, it was also observed that there is a perfect epitaxial relation between the substrate and the doped layers [11]. Thus, the FSGP is an attractive growth method to study fluorescent SiC due to the high quality material that the method produces.

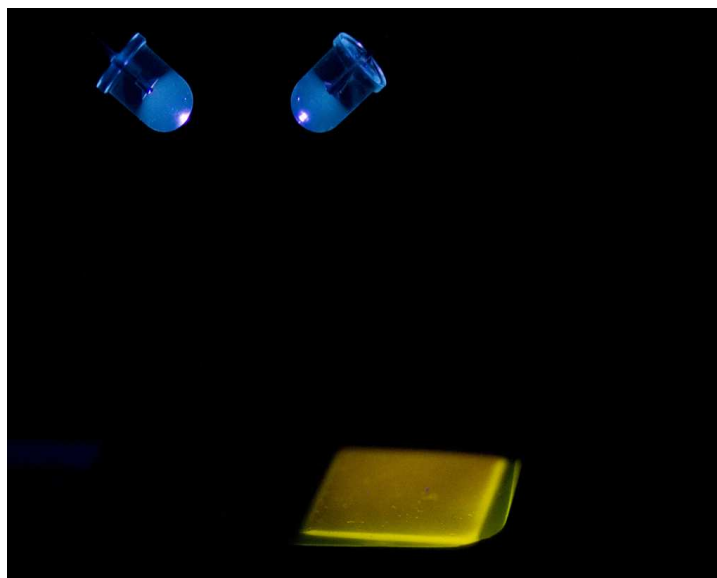


Fig. 13 N-B doped 6H-SiC that shows a luminescence even when excited by two weak ultraviolet LEDs.

At lower doping of nitrogen during the PVT growth, the steps seem to be fairly similar as demonstrated in growth on 4 degree off-oriented 4H-SiC substrates, Figure 14. There seems to be no pronounced influence on step-bunching or instabilities. It is likely that further increases in luminescence may be possible to obtain once the fundamental issues in growth and doping on the optical properties in fluorescent SiC are understood.

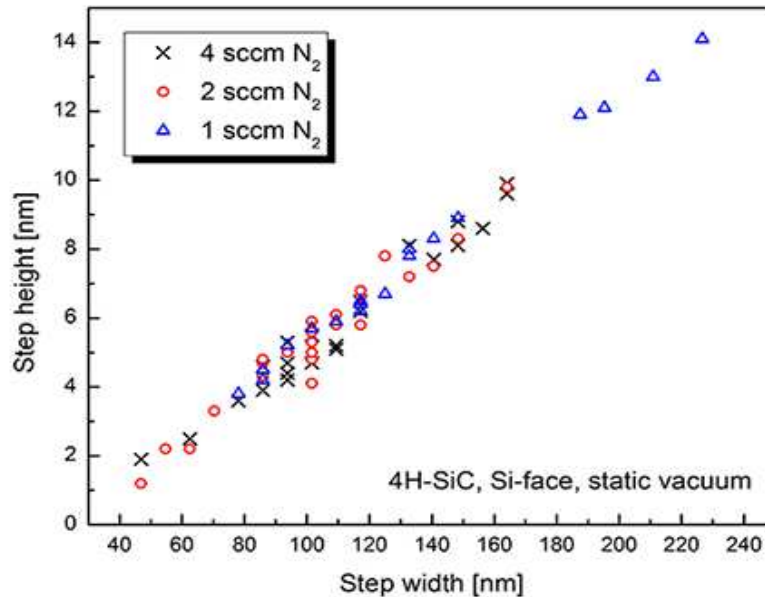


Fig. 14 Step width and step height in N-B doped 4H-SiC with source prepared with different nitrogen flows during PVT growth [25]

### 3.3 From inclusions to bulk: 3C-SiC and its photovoltaic potential

The sandwich configuration has many benefits. In particular, the high growth rate that is maintained as a benefit from the PVT growth mechanism is one interesting issue. This has shown that very thick layers may be produced. Also, the growth temperature is reduced compared with PVT. In fact, we have observed that 3C-SiC easily starts to nucleate. Figure 15 shows a repeated growth with initial 3C-SiC nucleation that expands upon further growth. Inclusions may appear also in the fluorescent silicon carbide layers, and it was shown that stacking faults appear in the 6H-SiC region close to the 3C-SiC [26]. The 3C-SiC inclusions, both in macroscopic and microscopic form, should be avoided since they will cause other radiation channels than in the donor to acceptor pair mechanism that is targeted.

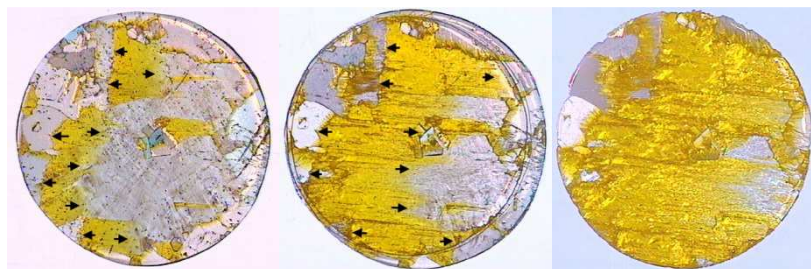


Fig. 15 Three consecutive growths on one and the same wafer with diameter of 20 mm. The 3C-SiC region clearly expand with increasing layer thickness [27]

In fact, by further growth and at higher growth rates, free standing and bulk-like 3C-SiC has shown to produce as high quality as 4H-SiC commercial substrates, Fig. 16 [28]. This is very interesting from an optoelectronic point of view. Cubic silicon carbide that is doped with boron fits very nicely in to the intermediate bandgap solar cell concept [29], which can be explored when the high quality material is possible to achieve.

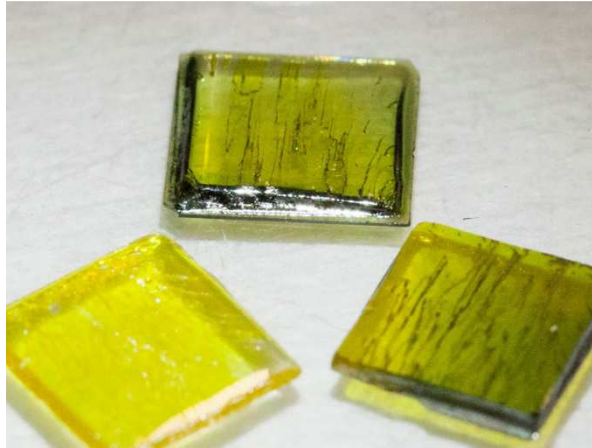


Fig.16 Three free standing 3C-SiC substrates with size 10x10 mm.

#### 4. Optical characterization of fluorescent SiC

With the application focus of SiC for light-emitting diodes, the FSGP grown 6H-SiC is characterized by using different technologies of photoluminescence and Raman spectroscopy in order to optimize its growth conditions for the wavelength conversion. A series of SiC samples (a, b, c, d and e) were grown with different B and N concentrations, and listed in Table 2. Details of the sample growth could be found in [30]. The concentration of the B and N are measured by using secondary ion mass spectroscopy (SIMS). For all the samples, the B concentration is in the order of  $10^{18} \text{ cm}^{-3}$ , while the N concentration increases dramatically from  $10^{16}$  to  $10^{18} \text{ cm}^{-3}$ .

**Table 2.** Dopant concentrations and normalized PL peak intensities of the samples

Sample	B concentration [ $\text{cm}^{-3}$ ]	N concentration [ $\text{cm}^{-3}$ ]	PL peak intensity [Normalized to sample d]
a	$8.0 \times 10^{18}$	$4.0 \times 10^{16}$	0.0 %
b	$6.9 \times 10^{18}$	$3.2 \times 10^{18}$	6.6 %
c	$6.9 \times 10^{18}$	$6.0 \times 10^{18}$	8.3 %
d	$4.4 \times 10^{18}$	$9.0 \times 10^{18}$	100 %
e	$5.2 \times 10^{18}$	$9.2 \times 10^{18}$	77.1 %

#### 4.1 Photoluminescence measurement [30]

The photoluminescence of the above 5 samples were measured by using an Olympus reflected fluorescence microscope system, a 377 nm diode laser as excitation source (focused by a 20X objective), and an Instrument System CAS 140B spectrometer. The integration time was 10 seconds with excitation power density of  $0.02 \text{ W/cm}^2$ , and the measurements were performed at room temperature.

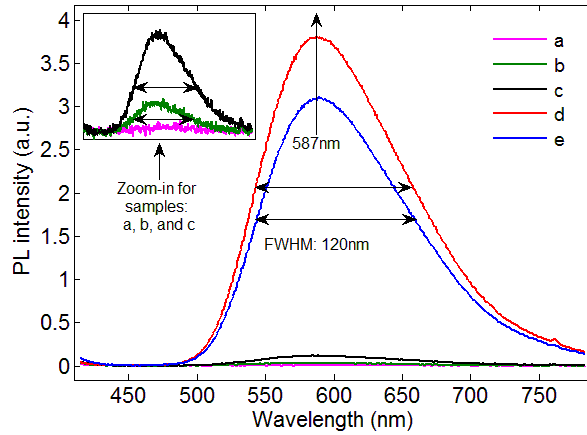


Fig. 17 Measured PL spectra of N-B co-doped 6H-SiC samples (inset: zoom-in for sample a, b, and c), same peak wavelength at 587 nm and FWHM of 120 nm were observed in all the spectra

As seen from Fig. 17, the PL intensity increases as the N concentration increases from sample a, over b and c, to sample d. Then the intensity starts to decrease when the N concentration increases further from sample d to sample e. In general, the photoluminescence is quite weak for p-type doping samples a, b and c, so their spectra have to be enlarged in order to see any features. Sample d and e show very intensive yellow fluorescence, illustrated in Fig. 17, compared to samples a, b, and c. According to the mechanism drawing in Fig.2, emission intensity increases as the dopants concentration increase, which is followed by sample a, b, c, and d. The deviation from sample d to sample e could be explained by the different ionization energy of donor and acceptor. For N and B, the concentration difference is of  $4.6 \times 10^{19} \text{ cm}^{-3}$  for the optimal sample.

#### 4.2 Raman spectroscopy [30]

Raman scattering spectra of the 6H-SiC samples were acquired in a backscattering configuration using the 514.5 nm line from an Ar ion laser (5 mW). The Raman spectra of the longitudinal optical phonon-plasmon coupled (LOPC) modes in the Raman spectra for 5 samples are shown in Fig. 18, and the mechanisms of Raman shifts in p- and n-type samples are different. The LOPC mode would broaden, lower its intensity, and shift toward higher wavenumbers with increasing free carrier concentrations. Usually, it is more sensitive to the amount of free electrons than to free holes.

In p-type samples, very few acceptor states are ionized due to the large ionization energy, and the Raman shift is mainly contributed to the atomic size effect. The B atoms usually occupy Si lattice positions in SiC. The inter-atomic distance of a Si-C bond is longer than that of a B-C bond due to the smaller atomic radius of B. The biaxial tensile stress will be released which results in a decrease of the phonon oscillation frequency. So the LOPC mode shifts toward smaller wavenumbers with higher B concentrations.

For the n-type samples, the predominant mechanism causing the Raman shift of the LOPC mode is the free carrier (electron) concentration. Although no obvious peak shift has been observed between sample d and e due to the relatively small concentration difference, the peak intensity of the LOPC mode decreases as expected when the free electron concentration increases from sample e to d. Furthermore, one can see from Fig. 18 that the LOPC modes of n-type samples occur at significantly higher wavenumbers than the p-type ones.

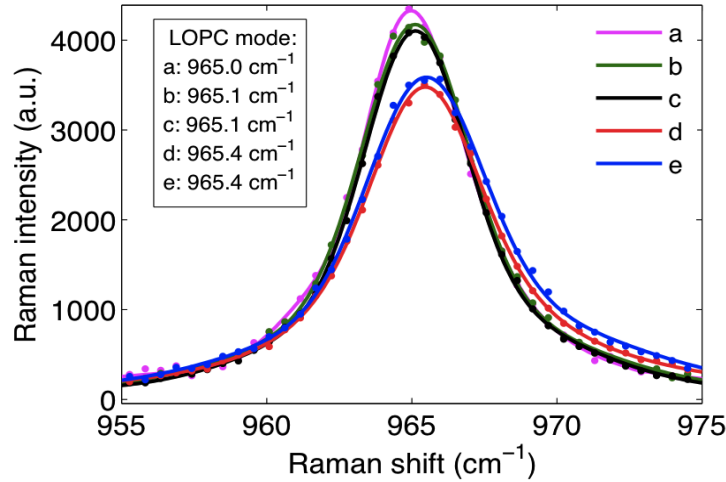


Fig.18 LOPC mode in Raman spectra (inset: positions of LOPC modes of the SiC samples with different dopant concentrations).

## 5. Light extraction enhancement for fluorescent SiC

Low extraction efficiency is a common problem for LED chips because the high refractive index of the semiconductor material confines most of the emitted light inside the device itself. It is challenging in the LED field to extract more light out of the device, therefore huge amount of effort has been made in the area to look for low-cost and effective solutions. Especially for fluorescent SiC based white LED, the SiC substrate has an even higher refractive index (2.65) than the sapphire substrate. Thus, it is a big issue to investigate. In this section, theoretical simulation is first made, in subsection 5.1, as guidance for the later experiments. In order to implement the simulated structures, a couple of nanostructuring methods have been applied with the intention to achieve low cost and high scalability without sacrificing the efficiency, in subsections 5.2 to 5.5.

In the following sub-sections, the dry etching of SiC is in RIE (STS cluster system C010). The optimal etching conditions, i.e. the radio frequency (R. F.) power (100 W), process pressure (30 mT), and gas flow rates (24 sccm SF<sub>6</sub>, 6 sccm O<sub>2</sub>), are used, unless otherwise stated. Surface reflectance measurements of different SiC samples were carried out by using a goniometer system (Instrument Systems, GON360). A halogen lamp as a broadband light source was connected to the transmitter arm of the goniometer and the receiver arm was connected to an optical spectrometer (Instrument Systems, CAS140B). The SiC samples were mounted on the sample stage and the reflection spectra were measured with an incidence angle of 8° with respect to the surface-normal direction.

Angle-resolved photoluminescence measurements were carried out by using the same goniometer. A 377 nm diode laser was connected to the transmitter arm as the excitation light source and the SiC sample was optically excited from its back side at room temperature. The detection angle of the receiver arm was varied from  $0^\circ$  (surface-normal direction) to  $85^\circ$  with a step of  $10^\circ$  and the corresponding photoluminescence spectra were then acquired.

### 5.1 Simulation [31]

The simulation is based on the two dimensional rigid coupled-wave analysis (2D-RCWA) algorithm, and both moth-eye and cylinder structures are arranged in the hexagonal grid.

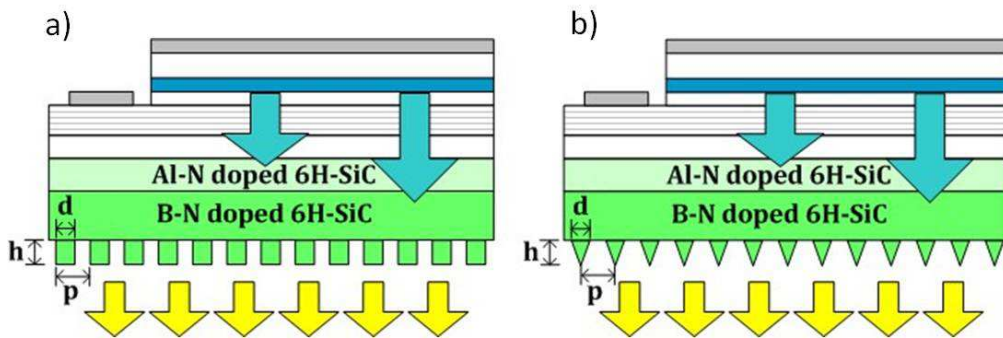


Fig.19 Schematic cross-section of modeled SiC-based white LED (a) with cylinder structures, (b) with moth-eye structures.

In both structures, the grating period is defined as  $p$  and is the distance between the centers of the neighboring structures,  $d$  is the width of the structure, and  $h$  is the height of the structure (illustrated in Fig. 19 a and 19b). Since the structure width has very weak influence on the light transmittance, fixed values of  $d=120$  nm and  $p=1.4d$  have been applied as the optimized profile in all the following simulations. The working wavelengths were set to the whole visible light range from 360 to 800 nm. Normal light incidence to the surface was applied for the simplification. The structure height was varied from 0 to 800 nm in steps of 5 nm.

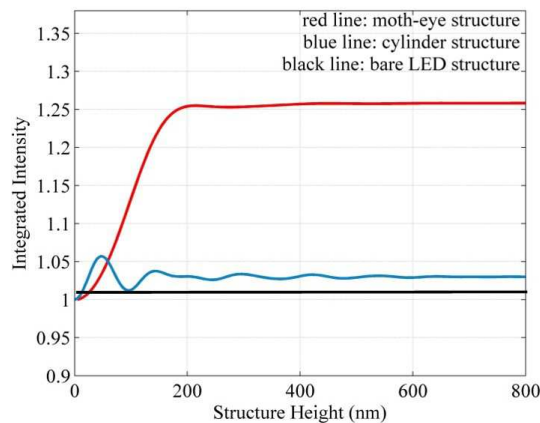


Fig.20 Integrated intensity of cylinder (blue line) and moth-eye structures (red line) as functions of the structure height.

All the calculated results are normalized to the one without any structure applied. It is obviously shown in Fig. 20 that moth-eye structure could improve the light extraction efficiency as high as 25%, which is much larger than the typical value of cylinder structure (2-3%). In order to reach as high as 25% extraction efficiency, the height of the cone structure should be larger than 180 nm, when the bottom diameter of the cone is 120 nm and the period of the cone is 168 nm. From the simulation, the nanocone structures are much better than the nanocylinder structures in term of enhanced transmittance. With this guidance, we have demonstrated experimentally the huge reflectance suppression and extraction efficiency enhancement in the following sub-sections.

## 5.2 Periodic nanostructures made by e-beam lithography [32]

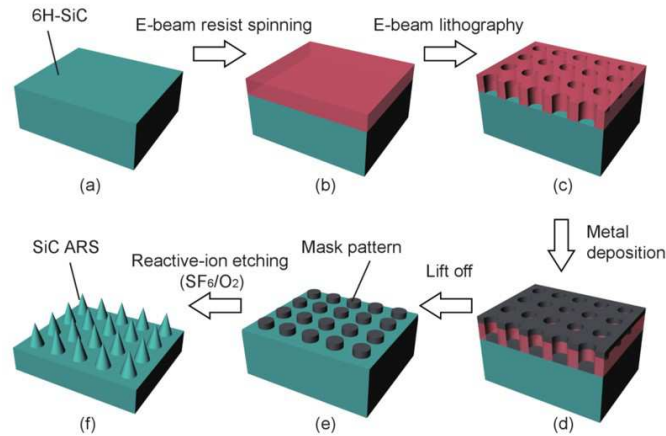


Fig. 21 Schematic illustrations of the SiC ARS fabrication process steps (a)-(f).

The periodic nanoconic anti-reflectance structures (ARS) are fabricated by using electron-beam lithography: Firstly, the positive e-beam resist (ZEP520) was spin-coated on the SiC sample (Fig. 21(a)) and then pre-baked on a hot plate at 160°C for 2 minutes (Fig. 21(b)). By using the e-beam writer (JEOL JBX9300FS) with a subsequent development process, the designed pattern was transferred to the e-beam resist coating (Fig. 21(c)). A hard mask material (chromium) layer was then deposited on the patterned SiC by the e-beam evaporation (Fig. 21(d)). Followed by a lift-off process, the dot-shaped pattern of chromium was obtained as a hard mask layer (Fig. 21(e)). The dry etching process using SF<sub>6</sub> and O<sub>2</sub> precursor gasses was carried out in the reactive ion etching (RIE) system. After 12 minutes etching, the cone-shaped ARS with designed configuration (bottom diameter of 240 nm, pitch of 340 nm, height of 1.2 μm, and hexagonal arrangement) were finally formed on the SiC surface (Fig.21(f)).

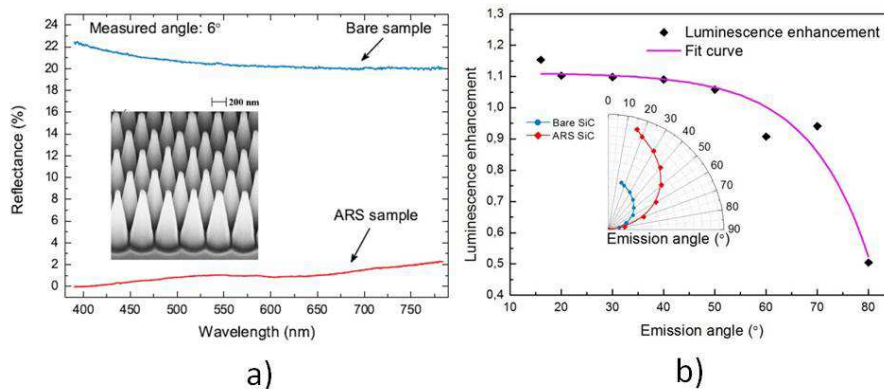


Fig. 22 (a) Surface reflectance (inset: SEM image of fabricated ARS on SiC) and (b) spatial emission pattern.

The surface with nanostructures exhibits a highly suppressed average reflection from 21.6% for bare surface to 1.6% for nanostructured sample (Fig. 22 (a)). The light emission enhancement is omni-directional and the enhancement is larger than 100% for emission angle smaller than  $50^\circ$  (Fig. 22 (b)).

### 5.3 Periodic nanostructures made by nanosphere lithography [33]

E-beam lithography is a slow, expensive and serial process, thus not suitable for mass-production. A potentially cost effective method, i.e. nanosphere lithography, is therefore investigated. The processing flow of the nanodome structures is shown schematically in Fig. 23 and their corresponding SEM images are shown in Fig. 24 respectively. Firstly, a monolayer hexagonal-close-packed array of polystyrene (PS) nanospheres with a diameter of 600 nm (size dispersion of 1 %) was formed on a pre-treated SiC sample surface by a self-assembly method (see Fig. 23(a).) Subsequently, the SiC sample was subjected to RIE for pattern transfer, where the PS nanospheres monolayer serves as an etching template (see Fig. 23(b)). The PS nanospheres are a unique template as they shrink during the etching. After 5 minutes etching, the nanospheres are consumed completely and SiC nanodome (ND) structures are achieved (see Fig. 23(c)). In addition, a 57 nm thick  $\text{Si}_3\text{N}_4$  coating with an intermediate refractive index ( $n=2.0$ ) between the value of air ( $n=1$ ) and 6H-SiC ( $n=2.65$ ) was deposited on top of the nanodome structures by plasma-enhanced chemical vapor deposition (PECVD, STS cluster system C010). The  $\text{Si}_3\text{N}_4$  coated nanodome (CND) structures further enhance the extraction efficiency just for the proof-of-concept, although the optimal refractive index and the thickness for this purpose should be 1.64 and 72.5nm, respectively. This cost-effective method has been approved to work by the surface reflectance measurement and photoluminescence measurement, shown in Fig. 25.

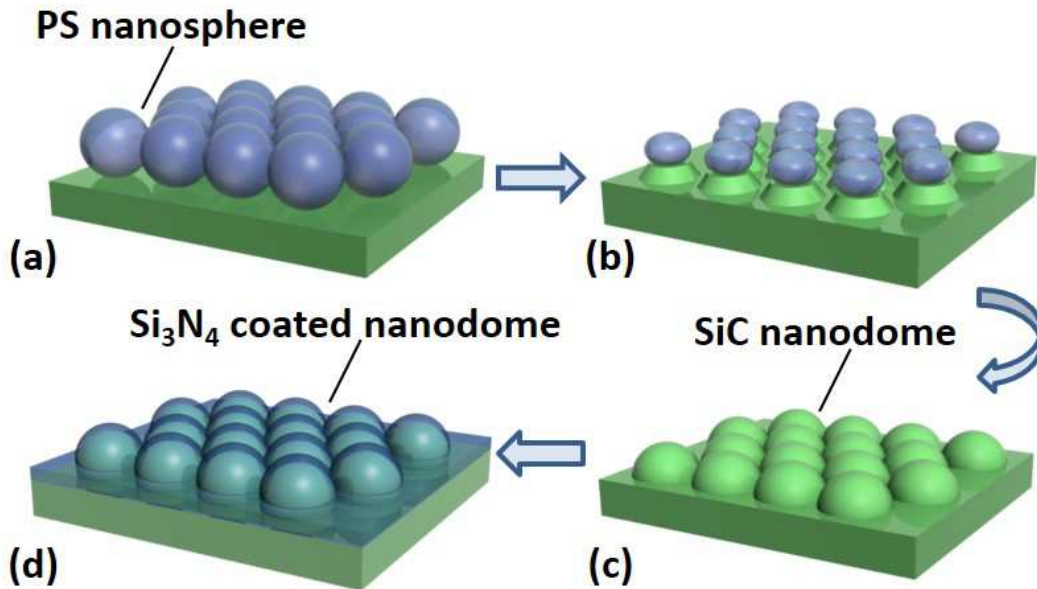


Fig. 23 Schematic diagram showing the detailed fabrication process of  $\text{Si}_3\text{N}_4$  coated nanodome structures on fluorescent SiC samples. (a) Formation of self-assembled polystyrene monolayer nanospheres as etching template, (b) dry etching process by RIE with  $\text{SF}_6$  and  $\text{O}_2$  gases, (c) formation of the nanodome structures on fluorescent SiC samples and, (d)  $\text{Si}_3\text{N}_4$  film deposition on SiC nanodome by PECVD.

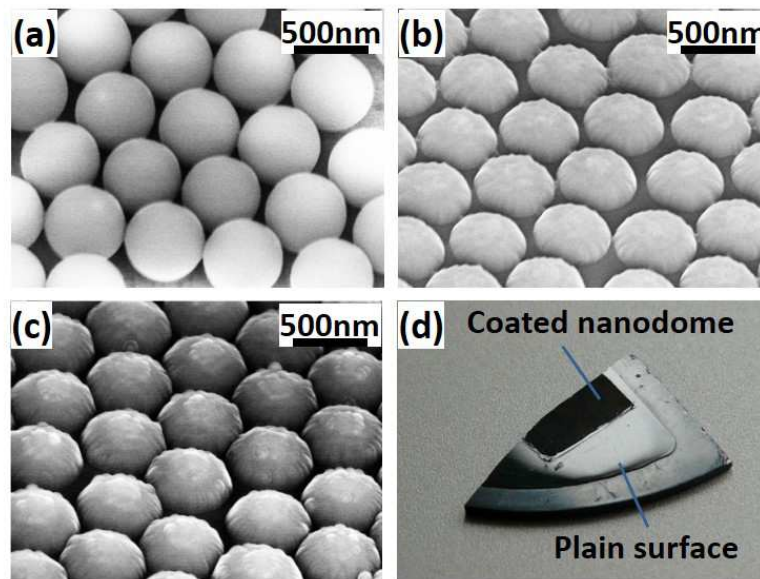


Fig. 24 Oblique-view SEM images of the (a) monolayer hexagonal-close-packed polystyrene nanospheres, (b) fabricated SiC nanodome structures, and (c)  $\text{Si}_3\text{N}_4$  coated nanodome structures respectively. (d) A photograph of SiC sample with a partially plain surface (lower right part) and partially covered by the coated nanodome structures (upper left part).

The measured reflectance spectra in a wavelength range of 390-785 nm are shown in Fig. 25(a). The average reflectance of plain-SiC is around 20.5%. Due to the graded refractive index profile of nanodomed (ND) SiC, the average reflectance is significantly suppressed to 2.0%. An even lower average reflectance of 0.99% is obtained for the coated nanodomed (CND) SiC sample. Fig. 25(b) shows that the fluorescent SiC sample exhibits a broad luminescence peaked at 575 nm and the luminescence is enhanced after surface nanostructuring. Compared to plain-SiC, the ND-SiC demonstrates a 107% luminescence enhancement. Meanwhile, the luminescence of the CND-SiC is enhanced significantly by 138%. The observed photoluminescence enhancement results are in a good consistency with the experimental observations from the surface reflectance suppression measurements.

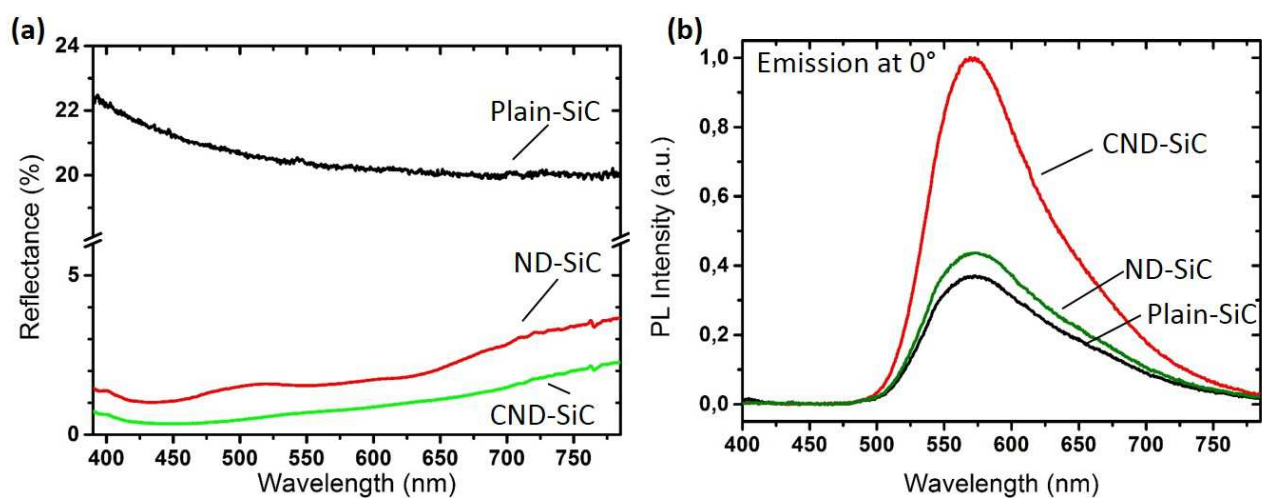


Fig. 25 (a) Surface reflectance suppression after the nanodome structuring and (b) Light extraction enhancement after the nanodome structuring.

## 5.4 Random nanostructures made by self-assembled metal nanoparticles [34-35]

Nanosphere lithography is not a standard LED fabrication process step. So it is difficult for this method to be adopted by the LED manufacturers. Therefore in addition to low cost and scalability, the new method should easily fit the current LED production line. Bearing this in mind, we developed a new method, i.e. using the self-assembled Au nano islands. The processing flow of this method is shown in Fig.26: a) a 10 nm Au film was deposited on the surface of SiC by e-beam evaporation; b) the sample was then heat treated in N<sub>2</sub> for 5 min at 350 degrees C and nano-islands were formed; c) the sample was then etched by reactive ion etching (RIE) using CF<sub>4</sub> and O<sub>2</sub> and nanocone structures were formed. One oblique-view SEM image of the formed nanocone structures is shown in Fig. 27(a). Their reflectance and photoluminescence are shown in Fig. 27(b) and (c) respectively with comparison to bare samples.

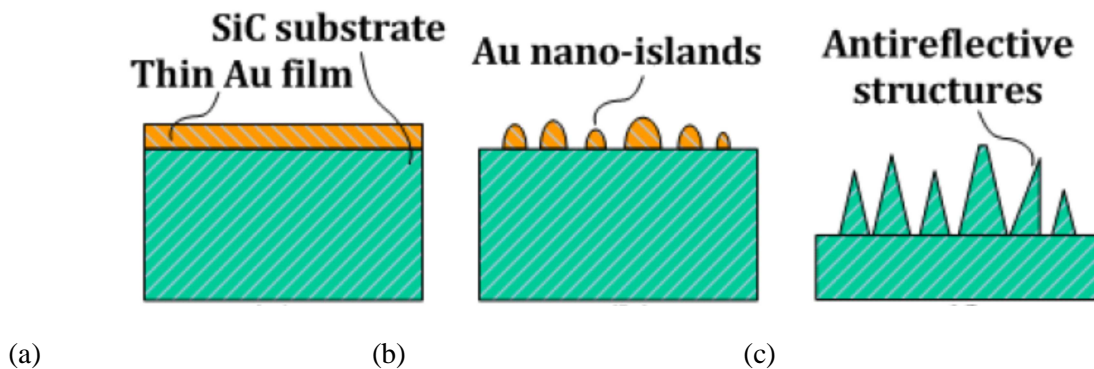


Fig. 26 Schematic illustrations of the SiC ARS fabrication process steps: (a) Au deposition; (b) Thermal treatment of Au thin films to form nano islands; (c) RIE etch to form the nanocones by using Au nano islands as mask.

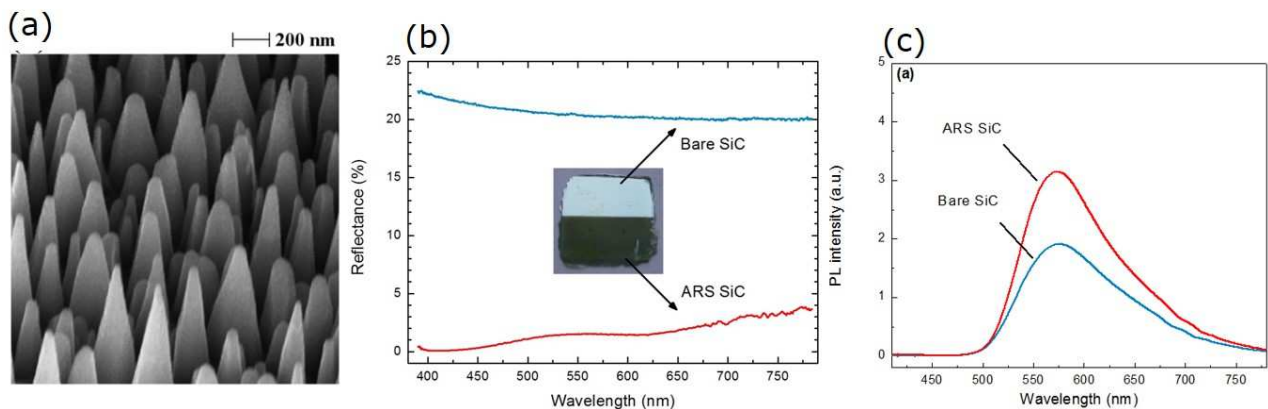


Fig. 27 (a) SEM image of the random nanocone structures, (b) Surface reflectance in the visible light range for both bare samples and ARS SiC. The inset is an optical microscope image of a sample, half surface turned black after the nanostructuring, (c) Photoluminescence enhancement of ARS sample, compared to bare SiC sample.

Figures 27 (b) and (c) show that the random nanostructures in this method is as good as the periodic ARS fabricated by e-beam lithography and nanosphere lithography. The reflectance is decreased to 1.6%, and the PL emission is enhanced by 67%.

### 5.5 Random nanostructures made by thin Al film [36]

The random nanostructures made by the self-assembled Au have demonstrated light extraction enhancement at the same level as the periodic structures, although with relatively simpler process and better scalability. However, the usage of Au in mass production is still not a cheap enough solution. Therefore, a new low-cost method is developed, which uses thin aluminium (Al) film as the etching mask to form nanostructures and could easily fit to the current LED production line.

The processing steps to fabricate the nanostructures consist of 40nm Al thin film deposition (Alcatel) and reactive ion etching as shown in Fig. 28. The processing details could be found from [36].

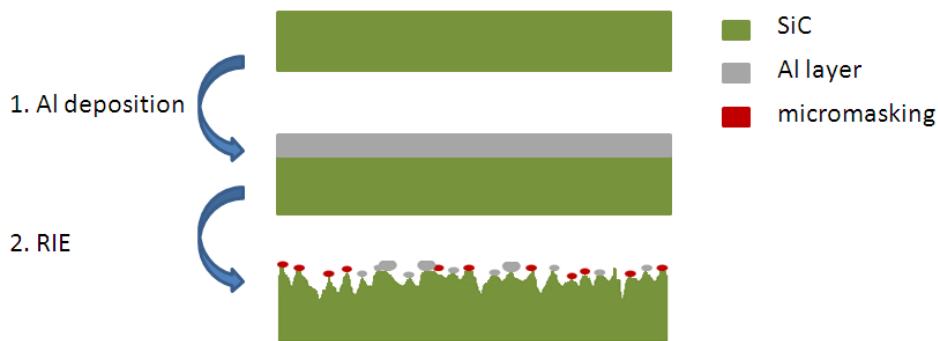


Fig. 28 Two-step processing to fabricate nanostructures using Al thin films: 1) Al deposition and 2) reactive ion etching.

Reflectance and photoluminescence measurements were performed on the nanostructured and bare f-SiC samples. The results for the reflectance of both bare sample and nanostructured sample are shown in Fig. 29. The insets are SEM images of the top-view and oblique view nanostructures. The reflectance has been dramatically suppressed from 22.5% for bare sample to 0.1% for the nanostructured sample.

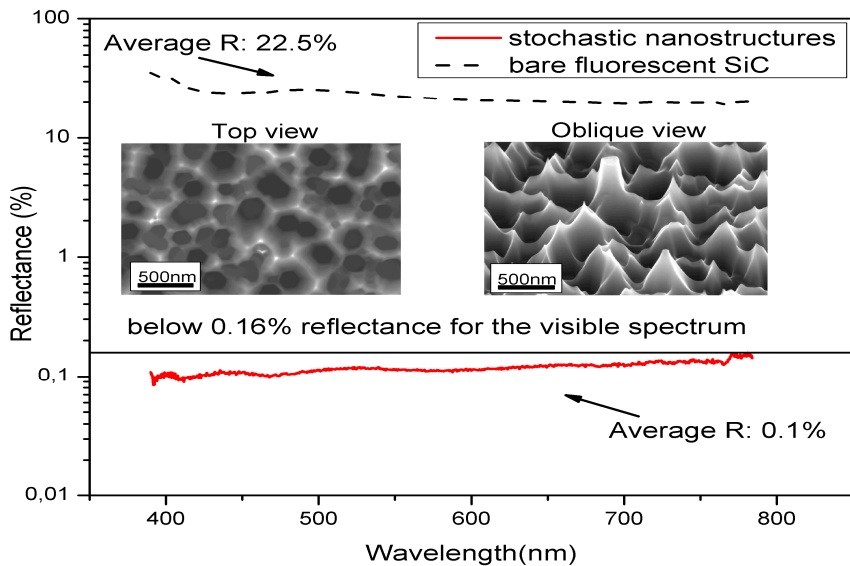
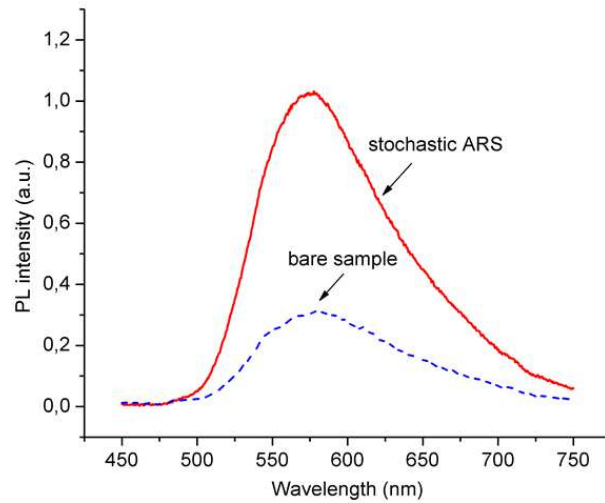


Fig. 29 Reflectance comparison between bare sample and nano-structured sample. The insets are SEM images of the f-SiC nanostructures (top view and oblique view)

As shown in Fig. 30, the photoluminescence of the sample with stochastic antireflection structures is enhanced by 210%, compared to that of the bare sample.



*Fig. 30 Photoluminescence comparison between bare f-SiC sample and nanostructured f-SiC sample*

## 6. Conclusions and perspectives

Apart from the many advantages SiC brings in the electronic devices, it is also emerging as a promising material for optoelectronic devices. In this paper we have reviewed the polycrystalline fluorescent SiC growth by PVT method, the single-crystalline SiC epitaxial growth by FSGP, as well as 4 different nanostructuring methods to enhance the extraction efficiency for the fluorescent SiC based white LEDs. The N-B codoped 6H-SiC has been demonstrated to be an ideal wavelength converter thanks to its good crystal-quality and high wavelength conversion efficiency.

Four different methods (periodic nanostructures by e-beam lithography and nanosphere lithography, random nanostructures by self-assembled Au nanoparticles and thin Al film) have been developed to enhance the extraction efficiency and substantial emission intensity increase has been demonstrated for all these different nanostructuring methods. It is expected that further improvement could be achieved when the surface passivation is investigated. These nanostructuring methods in one hand could enhance the light extraction efficiency for LEDs, and in the other hand could also increase the energy efficiency for solar cells.

Despite using SiC as a wavelength converter for white LED, high crystal quality SiC LED is also proposed to be a prospective room temperature source for single photons, a critical device for quantum telecommunication and information processing [37].

In addition to the application in LEDs, 3C SiC doped with B solar cell has been verified by simulation that its energy efficiency could reach as high as 48%, much higher than the 31% efficiency limit for single-junction Si solar cell. This so-called impurity photovoltaic effect has been proposed by Wolf since 1960 [38]. However, little experimental validation has been reported due to the poor crystal quality. As stated in section 2 and 3, we have now established a solid platform for the growth of crystalline SiC, and we hope to demonstrate this new concept experimentally.

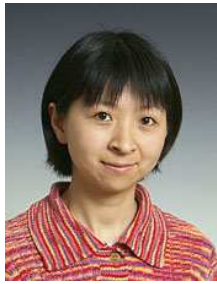
## Acknowledgment:

Financial support by the Danish councils for strategic research funding (no. 09-072118), Proof of Concept funding, Danish Ministry of Science, Innovation and Higher Education, Swedish energy agency, Nordic energy research, Swedish research council (no. 2009-5307), Ångpanneföreningen Research Foundation, Richerts Foundation. STAEDTLER Foundation (contract SH/eh 17/12) and BMBF (contract INNER 03SG0393) are gratefully acknowledged.

## References:

1. S. Kamiyama, T. Maeda, Y. Nakamura, M. Iwaya, H. Amano, I. Akasaki, H. Kinoshita, T. Furusho, M. Yoshimoto, T. Kimoto, J. Suda, A. Henry, I. G. Ivanov, J. P. Bergman, B. Monemar, T. Onuma, and S. F. Chichibu, *J. Appl. Phys.* **99**, 093108 (2006), DOI: 10.1063/1.2195883
2. P.T.B. Shaffer, *App. Optics* **10**, 1034 (1971), DOI: 10.1364/AO.10.001034
3. V. Jokubavicius, P. Hens, R. Liljedahl, J. W. Sun, M. Kaiser, P. Wellmann, S. Sano, R. Yakimova, S. Kamiyama and M. Syväjärvi, *Thin Solid Films* **522**, 7 (2012), doi:10.1016/j.tsf.2011.10.176
4. X. Bourrat, B. Trouvat, G. Limousin, G. Vignoles, F. Doux, *J. Mat. Res.* **15**, 92 (2000), DOI: 10.1557/JMR.2000.0017
5. T.L. Straubinger, M. Bickermann, R. Weingärtner, P.J. Wellmann and A. Winnacker, *J. Cryst. Growth* **240** (1-2), 117 (2002), DOI: 10.1016/S0022-0248(02)00917-X
6. P. Wellmann, P. Desperrier, R. Müller, T. Straubinger, A. Winnacker, F. Baillet, E. Blanquet, J M Dedulle, M. Pons, *J. Cryst. Growth* **275**, e555 (2005), DOI: 10.1016/j.jcrysgro.2004.11.070
7. M. Kaiser, T. Hupfer, V. Jokubavicius, S. Schimmel, M. Syväjärvi, Y. Ou, H. Ou, M. K. Linnarsson, P. Wellmann, *Mat. Sci. Forum* **740**, 39 (2013), DOI: 10.4028/www.scientific.net/MSF.740-742.39
8. M. Kaiser, S. Schimmel, V. Jokubavicius, M K. Linnarsson, H Ou, M. Syväjärvi and P. Wellmann, Nucleation and growth of polycrystalline SiC, accepted by *Materials Science Engineering B*
9. T. Hupfer, P. Hens, M. Kaiser, V. Jokubavicius, M.l Syväjärvi and P. J. Wellmann, *Mater. Sci. Forum*, **740-742**, 52(2013), DOI: 10.4028/www.scientific.net/MSF.740-742.52
10. Y. Kawai, T. Maeda, Y.Nakamura, Y.Sakurai, M. Iwaya, S. Kamiyama, H. Amano, I. Akasaki, M. Yoshimoto, T. Furusho, H. Kinoshita, H. Shiomi, *Mater. Sci. Forum* **527-529**, 263 (2006)
11. M.Syväjärvi, J.Müller,S.W. Sun, V.Grivickas, Y.Ou, V.okubavicius, P.Hens, M.Kaisr, K.Ariyawong , K.Gulbinas, P.Hens, R.Liljedahl, M.K. Linnarsson, S. Kamiyama, P.Wellmann, E. Spiecker, H.Ou, *Phys. Scripta* , **T148**, 014002 (2012), DOI: 10.1088/0031-8949/2012/T148/014002
12. F.H. Nicoll, *J. Electrochem. Soc.* **110** 1165 (1963), DOI: 10.1149/1.2425614
13. Y.A. Vodakov, E.N. Mokhov, M.G. Ramm, and A.D. Roenkov, *Kristall und Technik* **14**, 729 (1979), DOI: 10.1002/crat.19790140618
14. E.N. Mokhov, I.L. Shulpina, A.S. Treguva, and Yu.A. Vodakov, *Crystal Res. Tech.* **16**, 879 (1981)
15. T. Yoshida, Y. Nishio, S.K. Lilov, S. Nishino, *Mater. Sci. Forum*, **264-268**, 155 (1998), DOI: 0.4028/www.scientific.net/MSF.264-268.155
16. A. Kakanakova-Georgieva, Mike F. MacMillan, Shigehiro Nishino, Rositza Yakimova, E. Janzén, *Mater. Sci. Forum*, **264-268**, 147 (1998), DOI: 10.4028/www.scientific.net/MSF.264-268.147
17. M. Syväjärvi, R. Yakimova, M. F. MacMillan, M. Tuominen, A. Kakanakova-Georgieva, Carl G. Hemmingsson, Ivan G. Ivanov, E.Janzén, *Mater. Sci. Forum*, **264-268**, 143 (1998), DOI: 10.4028/www.scientific.net/MSF.264-268.143
18. M. Syväjärvi and R. Yakimova, *The Comprehensive Semiconductor Science & Technology (SEST)*, Pallab Bhattacharya, Roberto Fornari and Hiroshi Kamimura (Eds), ISBN 978-0-444-53144-5 (2011), p 202-231].
19. K. Shibahara, N. Kuroda, S. Nishino, and H. Matsunami, *Jap. J. Appl. Phys.* **26**, L1815 (1987)
20. T. Kimoto, A. Itoh, and H. Matsunami, *Appl. Phys. Lett.* **66**, 3645 (1995), DOI: 10.1063/1.114127
21. M. Syväjärvi, R. Yakimova, and E. Janzén, *J. Crystal Growth* **236**, 297 (2002), DOI: 10.1016/S0022-0248(01)02331-4

22. T. Kimoto, A. Itoh, H. Matsunami, and T. Okano, *J. Appl. Phys.* **81**, 3494 (1997), DOI: 10.1063/1.365048
23. N. Ohtani, M. Katsuno, J. Takahashi, H. Yashiro, and M. Kanaya, *Phys. Rev. B* **59**, 4592 (1999), DOI:10.1103/PhysRevB.59.4592
24. M. Syväjärvi, R. Yakimova, H. Jacobsson, and E. Janzén, *J. Appl. Phys.* **88**, 1407 (2000)
25. S. Schimmel, M. Kaiser, P. Hens, V. Jokubavicius, R. Liljedahl, J. Sun, R. Yakimova, Y. Ou, H. Ou, M.K. Linnarsson, P.J. Wellmann, M. Syväjärvi, *Mater.Sci.Forum* **740-742**, 185 (2013), DOI: 10.4028/www.scientific.net/MSF.740-742.185
26. J. W. Sun, T. Robert, A. Andreadou, A. Mantzari, V. Jokubavicius, R. Yakimova, J. Camassel, S. Juillaguet, E. K. Polychroniadis, and M. Syväjärvi, *J. Appl. Phys.* **111**, 113527 (2012), DOI: 10.1063/1.4729064
27. M. Syväjärvi, R. Yakimova, H. Jacobsson, and E. Janzén, *Mater. Sci. Forum* **353-356**, 143 (2001)
28. J. W Sun, I.G. Ivanov, R. Liljedahl, R. Yakimova and M. Syväjärvi, *Appl. Phys. Lett.* **100**, 252101/1-4 (2012), DOI: 10.1063/1.4729583
29. M. Syväjärvi, *Adv. Mat. Lett.* **3**, 175 (2012)
30. Y. Ou, V. Jokubavicius, S. Kamiyama, C. Liu, R. W Berg, M. Linnarsson, R. Yakimova, M. Syväjärvi, H. Ou, *Opt. Mater. Express*, **1**, 1439 (2011)
31. Y. Ou, D. D. Corell, C. Dam-Hansen, P. M. Petersen, H. Ou, *Opt. Express*, **19**, A166, (2011)
32. Y. Ou, V. Jokubavicius, P. Hens, M. Kaiser, P. Wellmann, R. Yakimova, M. Syväjärvi, and H. Ou, *Opt. Express* **20**, 7575 (2012)
33. Y. Ou, X. Zhu, U. Møller, S. Xiao, and H. Ou, 'Broadband antireflection nanodome structures on SiC substrate', Group IV photonics, WP3, Soul, Korea (2013)
34. Y. Ou, I. Aijaz, V. Jokubavicius, R. Yakimova, M. Syväjärvi, and H. Ou, *Opt. Mater. Express* **3**, 86 (2013)
35. Y. Ou, V. Jokubavicius, R. Yakimova, M. Syväjärvi, H. Ou, *Opt. Lett.*, **37**, 3816 (2012)
36. A. Argyraki, Y. Ou, H. Ou, *Opt. Mater. Express*, **3**, 1119 (2013)
37. F. Fuchs, V. A. Soltamov, S. Vaeth, P. G. Baranov, E. N. Mokhov, G. V. Astakhov, V. Dyakonov, *Sci. Rep.* **3**, 1637 (2013) DOI: [10.1038/srep01637](https://doi.org/10.1038/srep01637)
38. M. Wolf, in *Proceedings of the IRE* [0096-8390] 1960, 48 p.1246



**Haiyan Ou** received the PhD degree in semiconductor devices and microelectronics from the Institute of Semiconductors, Chinese Academy of Sciences in 2000. From 2000, she joined Technical University of Denmark, where she was promoted as associate professor in 2005. She has been a JSPS (Japanese Society for Promotion of Science) fellow at Meijo University (Japan), and a visiting professor at the Institute of Semiconductors, CAS (China). Her scientific background is in the areas of materials and devices for optical communication, photovoltaics, and light emitting. She has published more than 120 journal and conference papers, and is the founder of Light Extraction ApS.



**Mikael Syväjärvi** received a PhD degree in materials science from Linköping University, Sweden in 1999. His expertise is in materials growth and technologies of SiC, graphene and related materials. He initiated a European research collaboration in fluorescent and photovoltaic SiC, and has co-organized several symposiums at E-MRS. He has published more than 200 journal and conference papers. He is a co-inventor of The Cubic Sublimation Method for cubic SiC and the Fast Sublimation Growth Process that is applied for industrial development of fluorescent hexagonal SiC. He is also co-inventor of the High Temperature Graphene Process and a co-founder of Graphensic AB that manufactures and supplies graphene on SiC.



**Peter Wellmann** received a PhD degree in materials science from University of Erlangen, Germany in 1995. From 1996 to 1998 he spent two years as PostDoc at the materials Department of the University of California in Santa Barbara, USA. Back in Germany he continued his research at the University of Erlangen, Germany, where he passed habilitation in 2001 and became a professor in 2006 / 2007. In 2004 and 2006 he spent several months as invited professor in Grenoble and Montpellier, France. His expertise is in materials science, technology (bulk growth and epitaxy) and characterization of compound semiconductor materials, in particular SiC, GaN, ITO, CIS/CZTS. He has published more than 140 journal and conference papers.